

Hadron-Quark Crossover and Massive Hybrid Stars

Kota Masuda

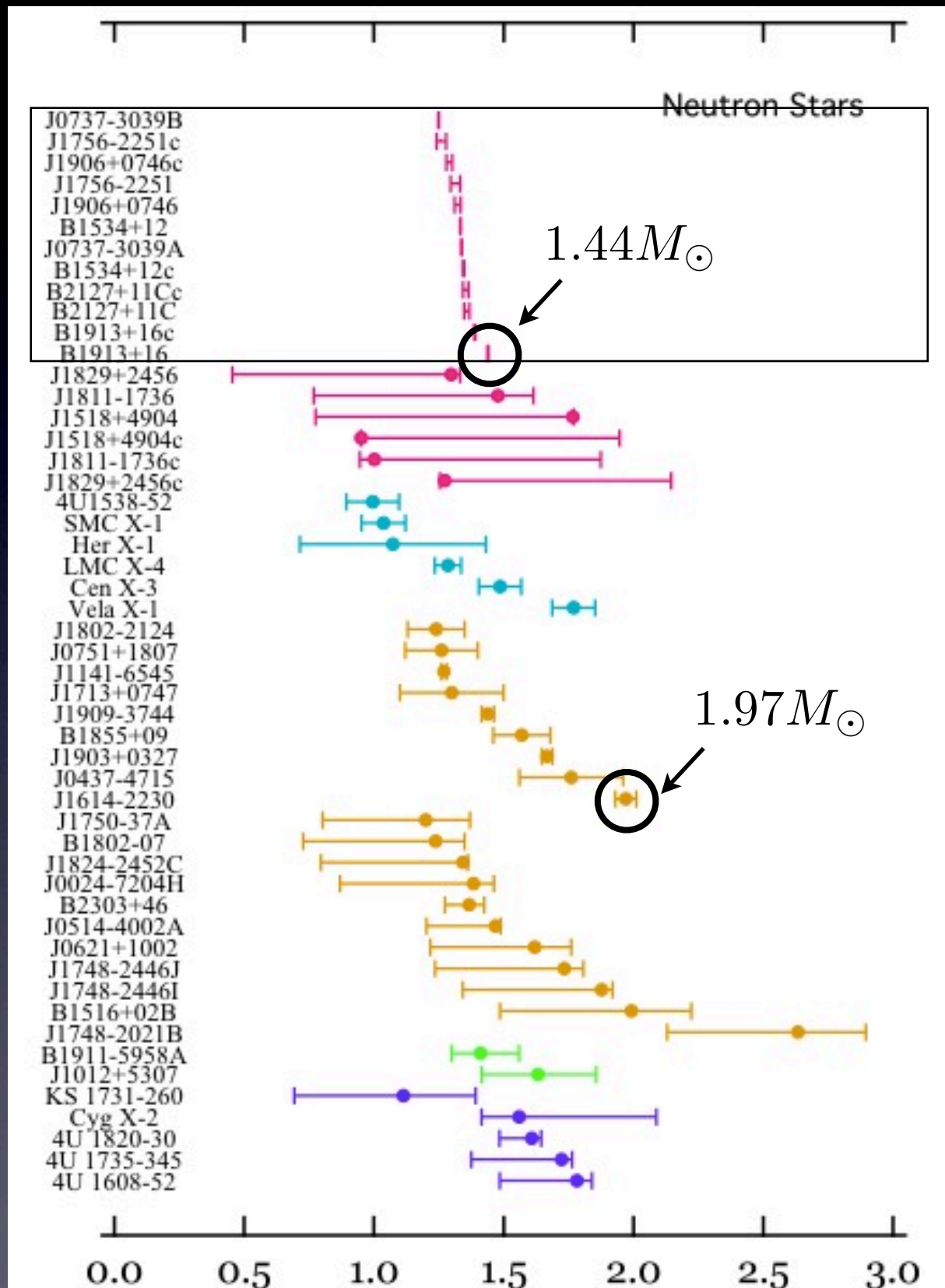
with Tetsuo Hatsuda (RIKEN) and Tatsuyuki Takatsuka (RIKEN)

[1] ``Hadron-Quark Crossover and Massive Hybrid Stars with Strangeness'',
Masuda, Hatsuda and Takatsuka, ApJ **764**, 12 (2013)

[2] ``Hadron-Quark Crossover and Massive Hybrid Stars'',
Masuda, Hatsuda and Takatsuka, PTEP 073D01 (2013)

Introduction: Massive Neutron Star

1/16

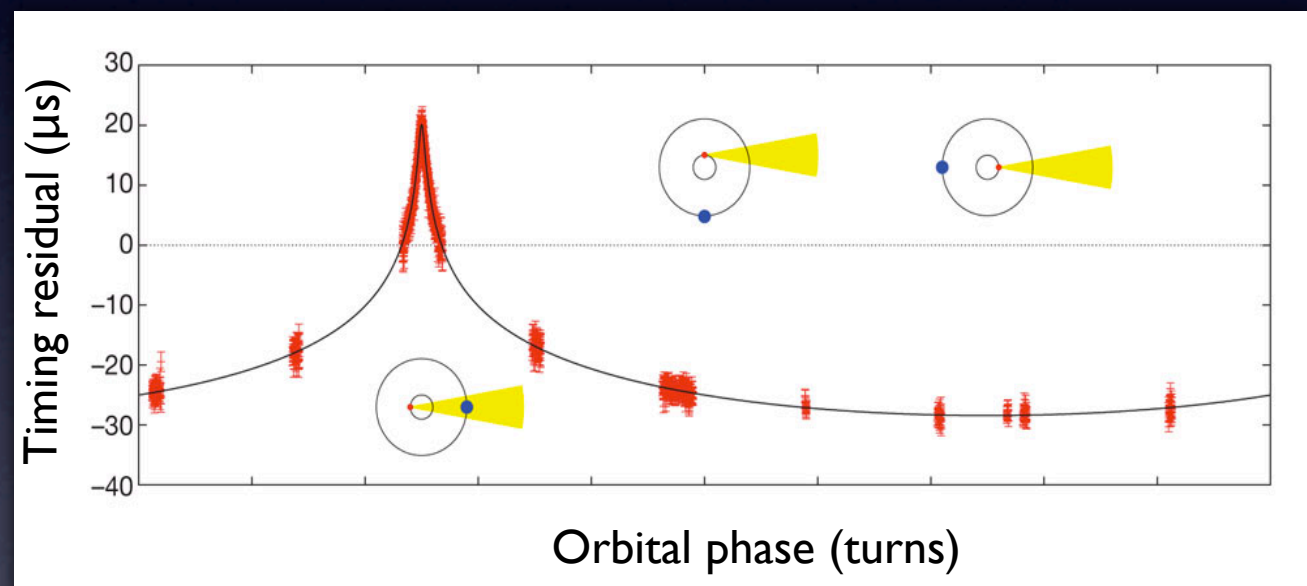


Typical value of the observed mass for double NS binaries $\sim 1.4M_{\odot}$



In 2010, NS (PSR J1614-2230, NS-WD binary) with $M = (1.97 \pm 0.04)M_{\odot}$ was found

Shapiro delay



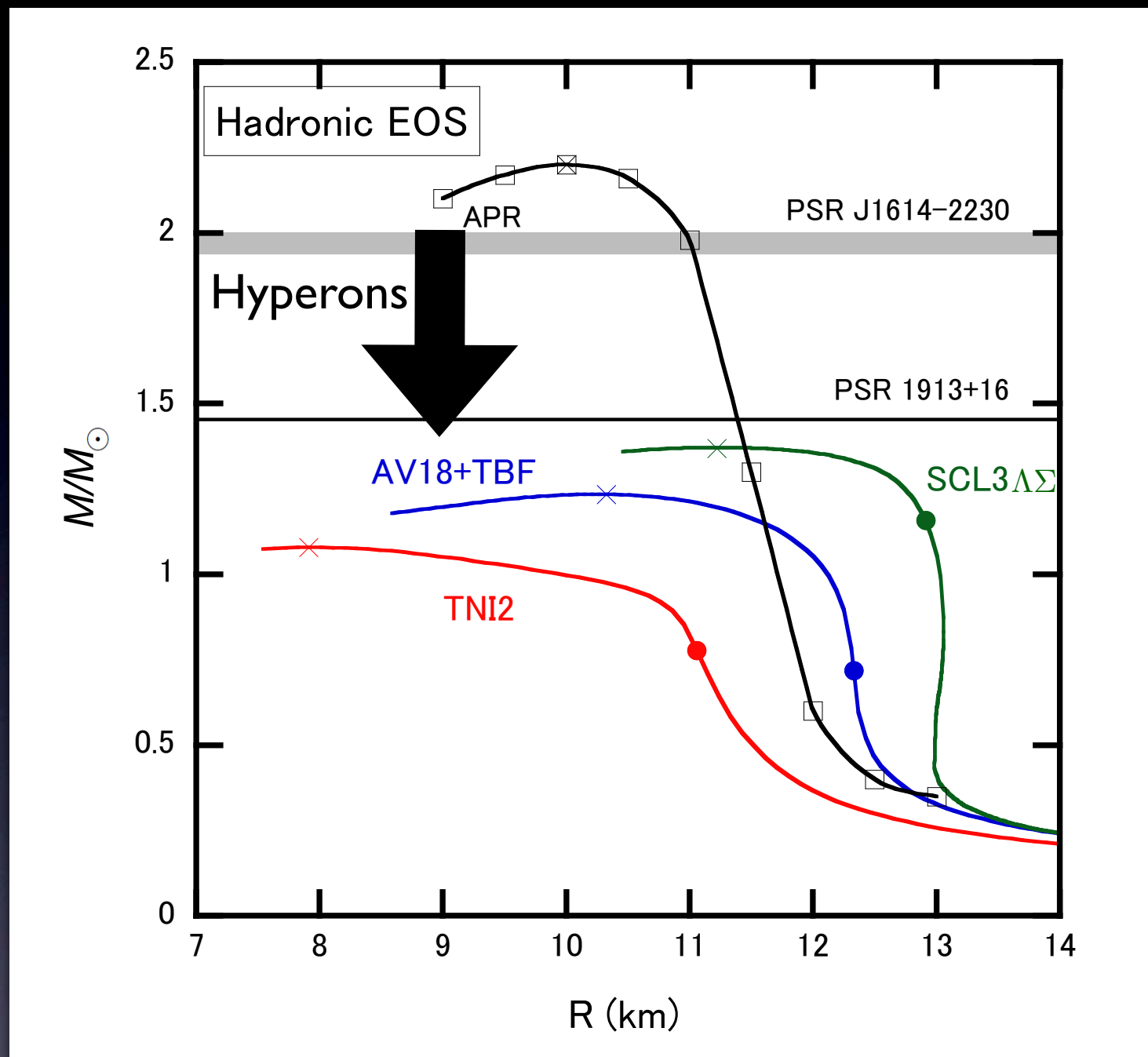
Key Questions:

Any EOS which can explain $2M_{\odot}$ NS?

The fate of the quark matter inside a heavy NS?

Hadronic EOSs

2/16



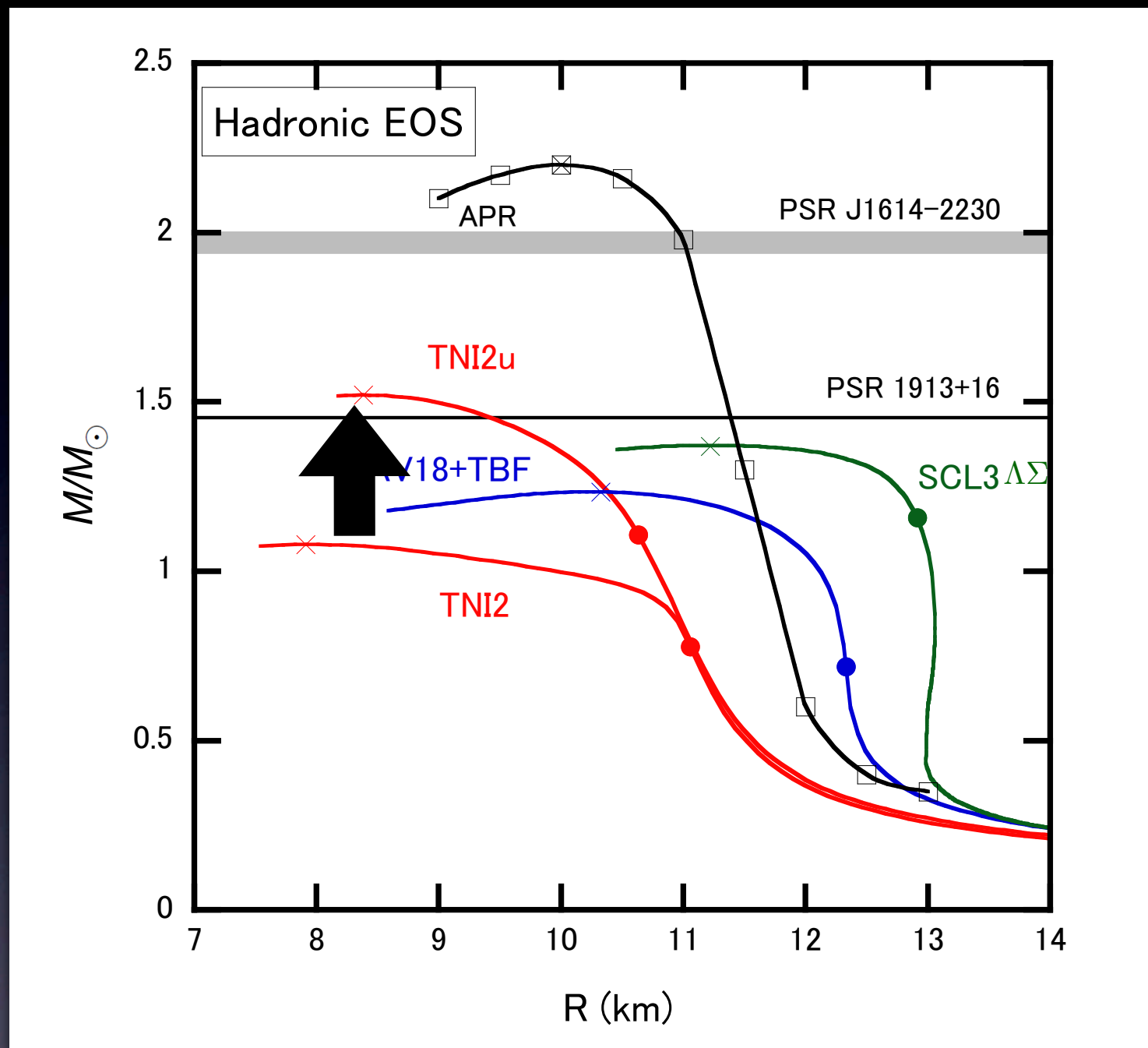
	(1) AV18+TBF	(2) TNI2	(3) SCL3 $\Lambda\Sigma$
Method	BHF	BHF	RMF
2NF	AV18	Reid	
3NF	Yes	Yes	No
Hyperons	Yes	Yes	Yes

- (1) Baldo *et al.* (2000), Schulze *et al.* (2010)
- (2) Nishizaki *et al.* (2001,2002)
- (3) Tsubakihara *et al.* (2010)

- Hyperons soften EOS \longrightarrow Maximum mass is less than $1.44M_\odot$.

Hadronic EOSs

2/16

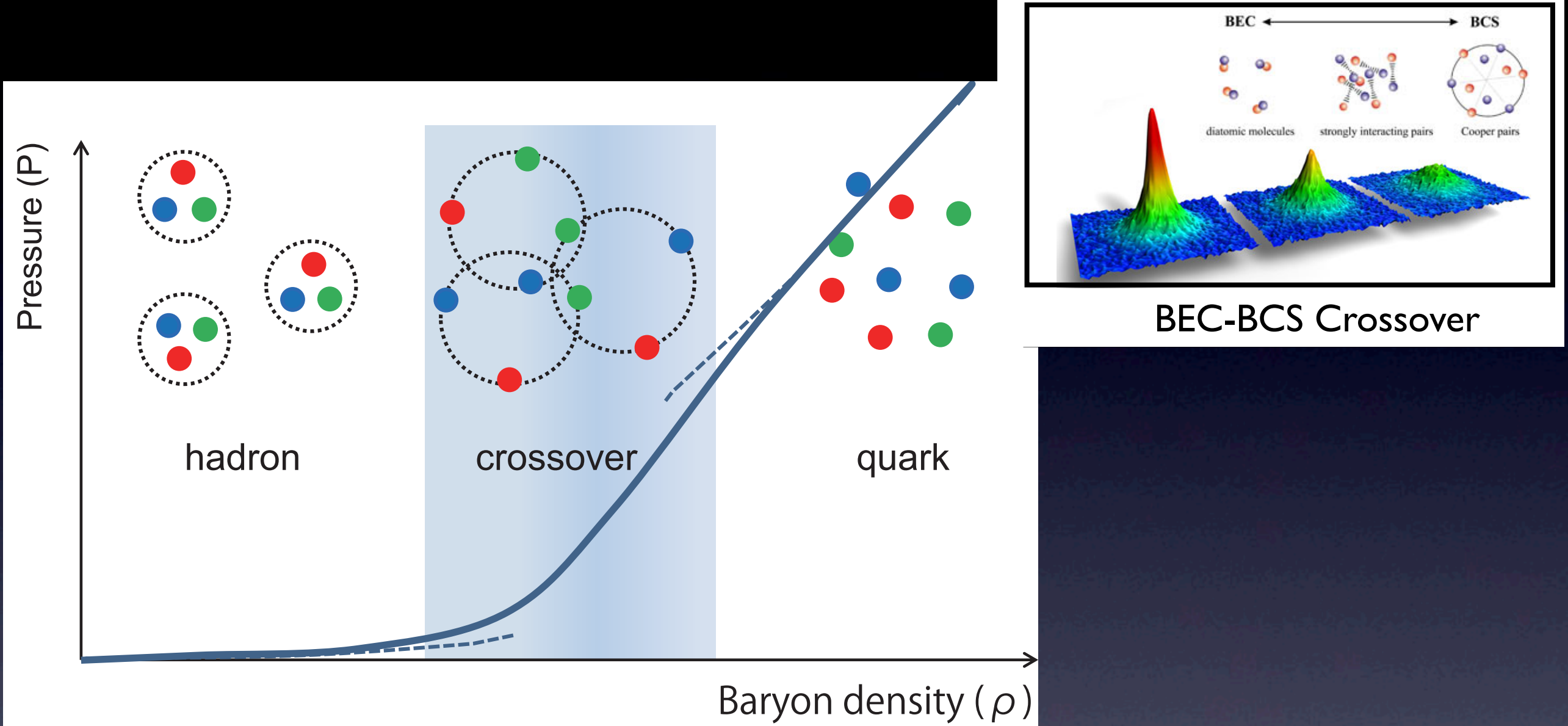


	TNI2	TNI2u
``NNN''	Yes	Yes
``NNY''		
``NYY''	No	
``YYY''		Yes

- Universal 3-body force stiffens EOS \longrightarrow Maximum mass is larger than $1.44M_\odot$.
- However maximum mass cannot exceed $2M_\odot$.

Hadron-Quark Crossover

3/16



This research seeks the possibility of crossover

Ref.)

Baym (1979)

Celik, Karsch and Satz (1980)

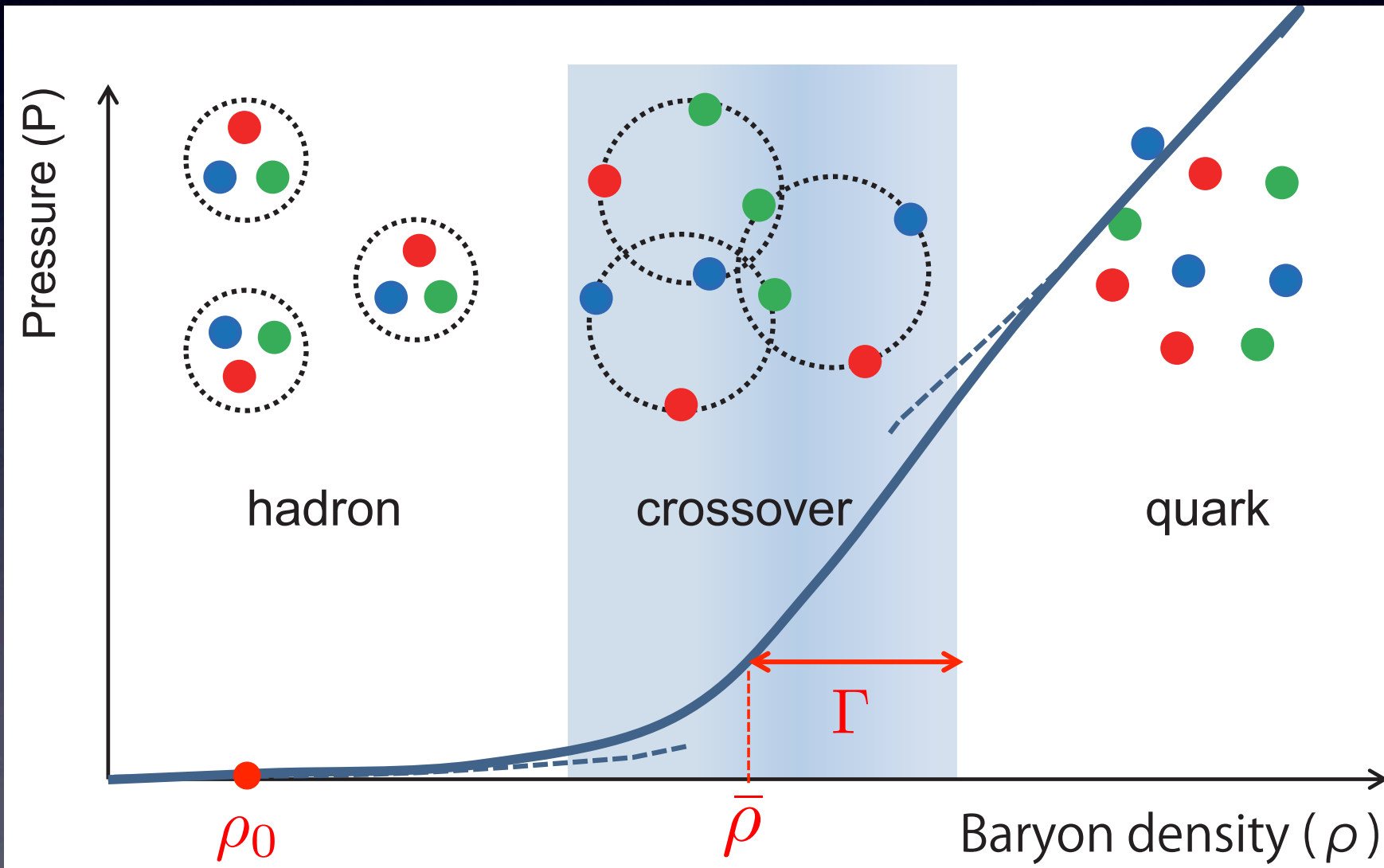
Fukushima (2004)

Hatsuda, Tachibana, Yamamoto and Baym (2006)

Method of Interpolation

Phenomenological interpolation: $P(\rho)$

$$\begin{cases} P = p_H \times f_- + p_Q \times f_+ & f_{\pm} = \frac{1 \pm \tanh(\frac{\rho - \bar{\rho}}{\Gamma})}{2} \\ P = \rho^2 \frac{\partial(\varepsilon/\rho)}{\rho} \end{cases}$$



Condition for $\bar{\rho}$: $f_+ < 0.1$ at $\rho_0 \rightarrow \bar{\rho} > \rho_0 + 2\Gamma$

EOS at $\rho \gg \bar{\rho}$

(2+1)-flavor NJL Lagrangian (u,d,s, e^- , μ^-)

$$L_{NJL} = \bar{q}(i\cancel{D} - m)q + \frac{G_s}{2} \sum_{a=0}^8 [(\bar{q}\lambda^a q)^2 + (\bar{q}i\gamma_5\lambda^a q)^2] - \frac{g_v}{2}(\bar{q}\gamma^\mu q)^2 + G_D[\det\bar{q}(1 + \gamma_5)q + \text{h.c.}]$$

Parameter set

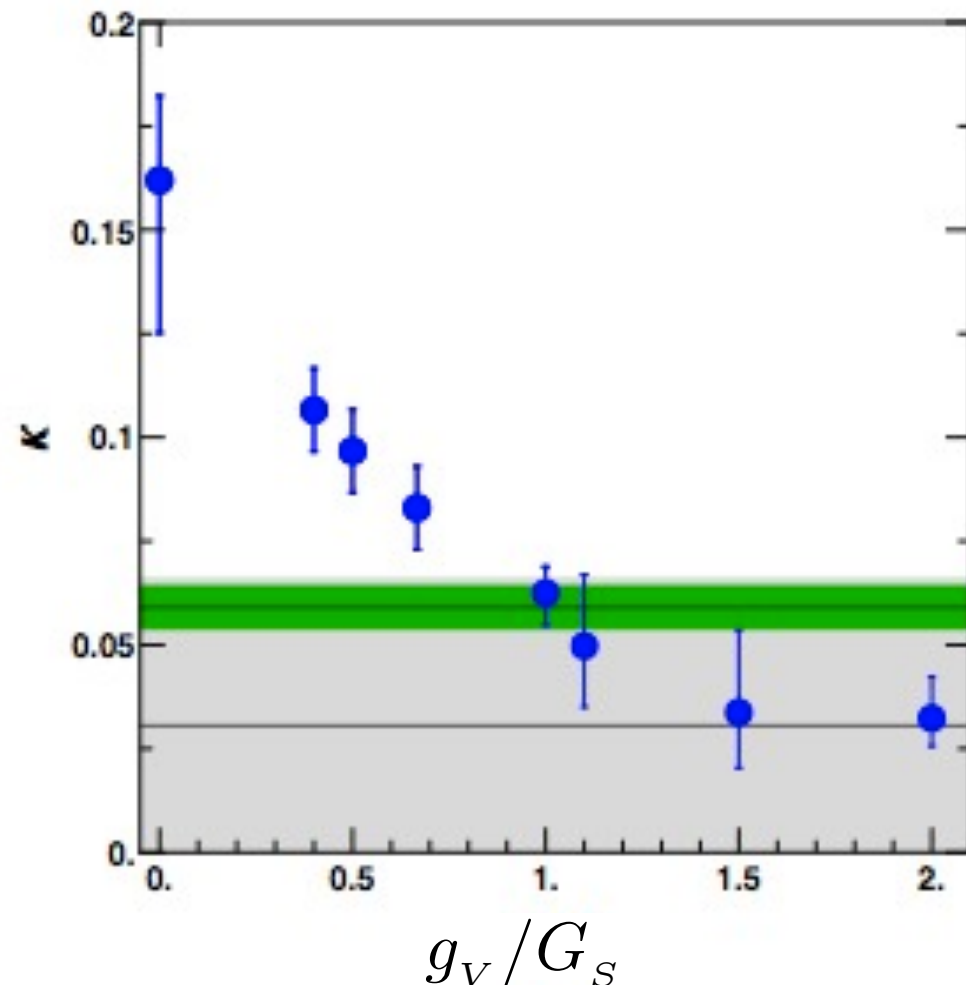
cutoff (MeV)	$G_s\Lambda^2$	$G_D\Lambda^5$	$m_{u,d}(\text{MeV})$	$m_s(\text{MeV})$
631.4	3.67	9.29	5.5	135.7

Hatsuda and Kunihiro (1994)

$$0 \leq g_v \leq 1.5G_s$$

Conditions:
 1. beta-equilibrium
 2. charge neutrality

Recent estimate of g_V



$$\kappa = -T_c \frac{d^2 T_c(\mu)}{d\mu^2} \Big|_{\mu^2 = 0}$$

$$\longrightarrow g_V \sim G_S$$

$g_V \geq 0$: repulsive

$g_V/G_S = 0$: no-repulsion

$g_V/G_S = 1.0$: medium repulsion

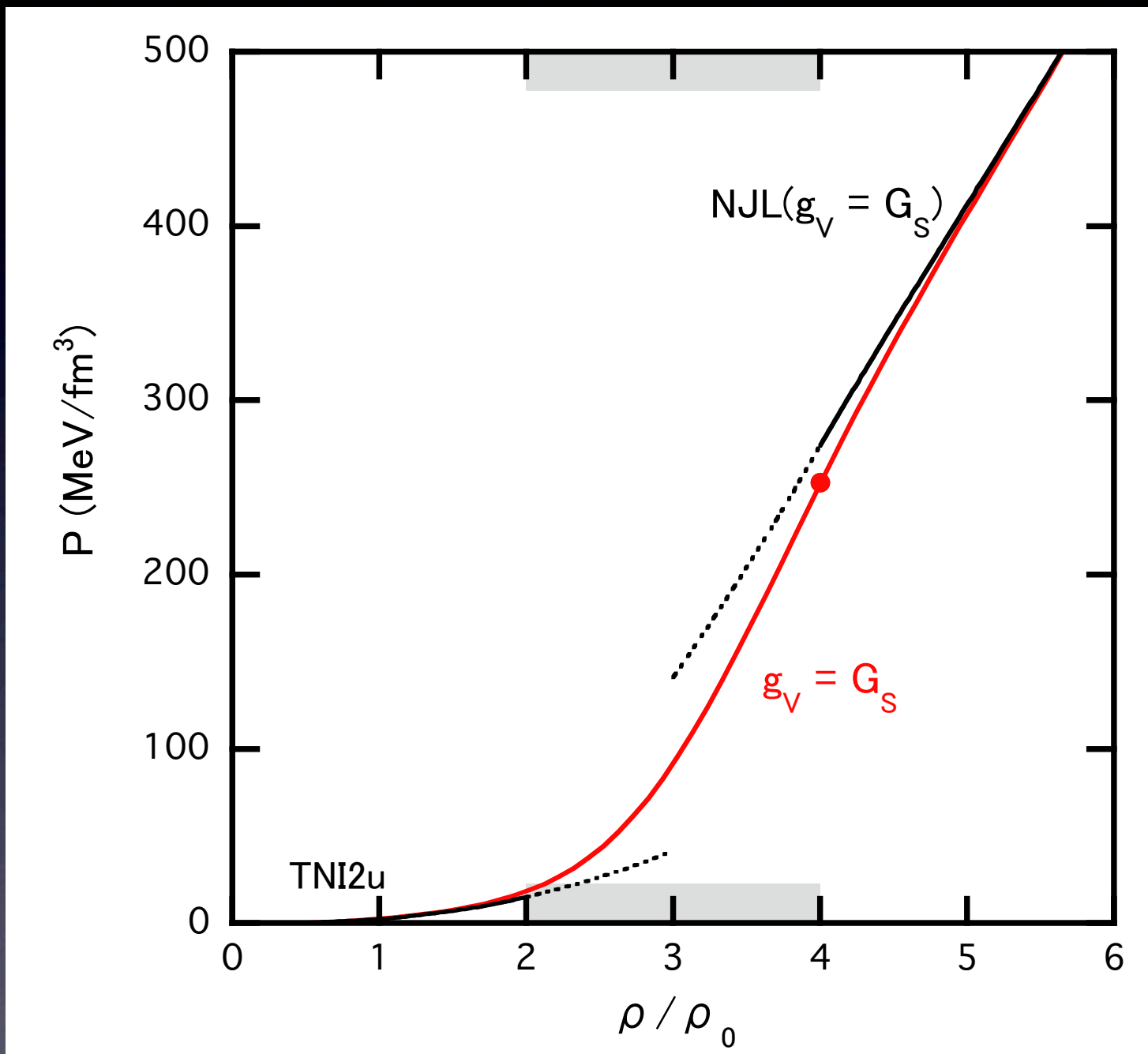
$g_V/G_S = 1.5$: strong repulsion

Interpolated EOS

6/16

H-EOS: TNI2u, Q-EOS: NJL

$$g_v = G_S \quad (\bar{\rho}, \Gamma) = (3\rho_0, \rho_0)$$

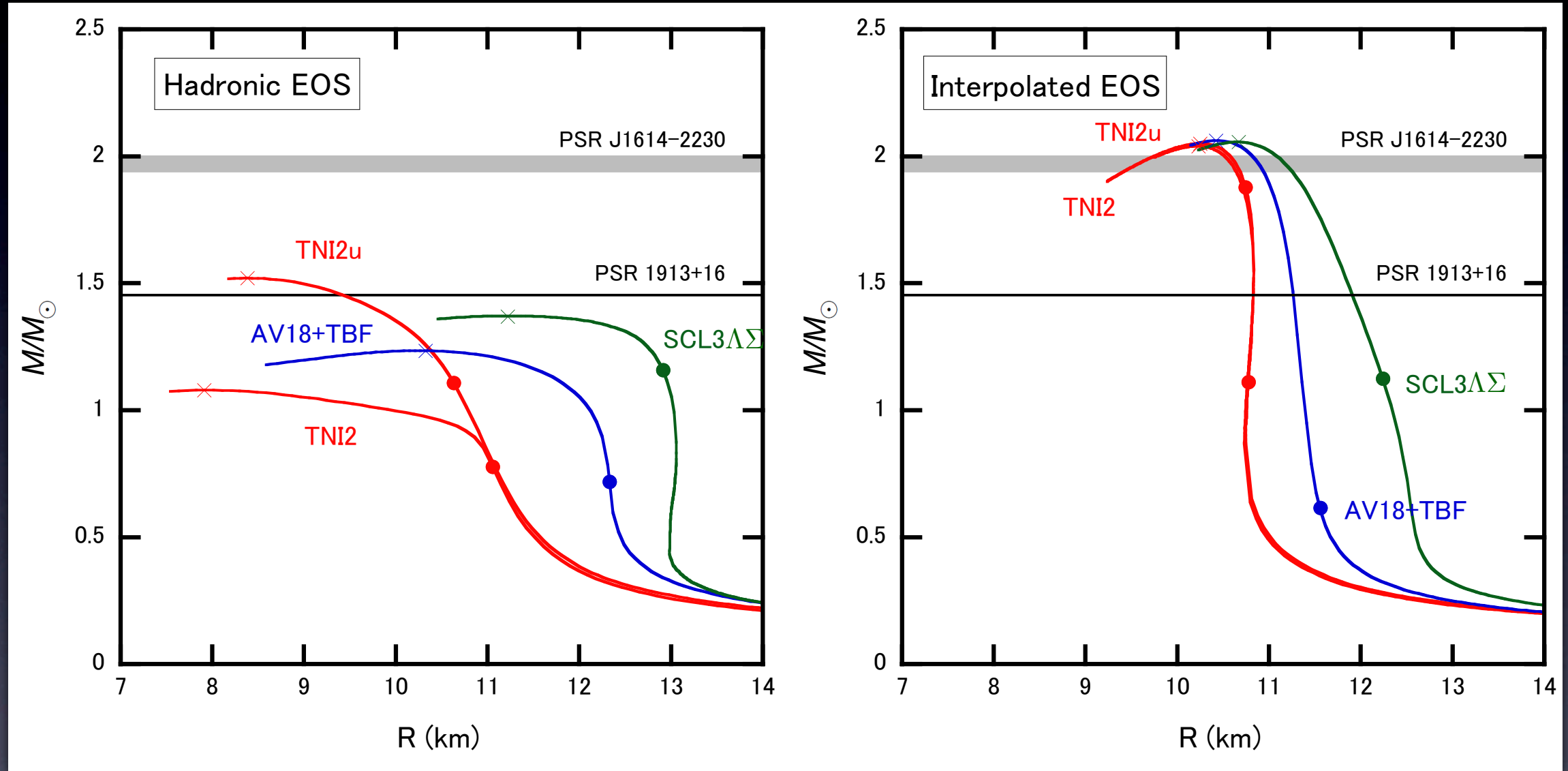


- In the crossover region, interpolated EOS is larger than H-EOS.
- Rapid stiffening of the EOS in the crossover region

Results (I): Effects of Q-EOS

7/16

M-R relation $(\bar{\rho}, \Gamma) = (3\rho_0, \rho_0)$ $g_v = G_S$



- Maximum mass exceeds 2 solar mass, no matter what kind of H-EOS is taken

Results (2): Effects of parameters

8/16

How maximum mass depends on $\bar{\rho}$, Γ

$\bar{\rho}$	$\Gamma/\rho_0 = 1$		$\Gamma/\rho_0 = 2$	
	$g_v = G_s$	$g_v = 1.5G_s$	$g_v = G_s$	$g_v = 1.5G_s$
$3\rho_0$	2.05	2.17	-	-
$4\rho_0$	1.89	1.97	-	-
$5\rho_0$	1.73	1.79	1.74	1.80
$6\rho_0$	1.60	1.64	1.62	1.66

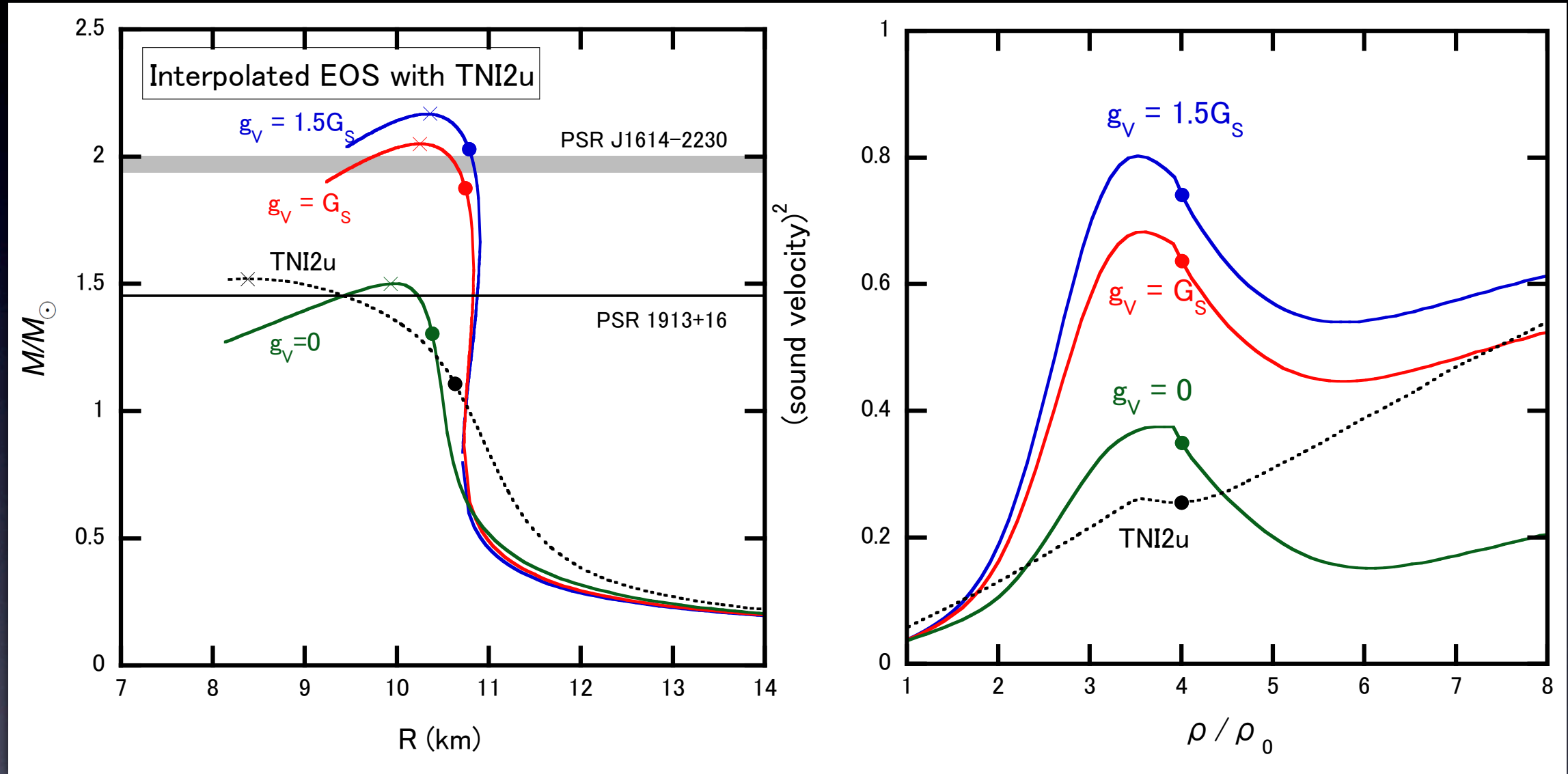


Crossover occurs at relatively low densities and quarks are strongly interacting $\rightarrow 2M_\odot$

Results (3): Sound Velocity

9/16

M-R relation $(\bar{\rho}, \Gamma) = (3\rho_0, \rho_0)$ $g_v = G_S$

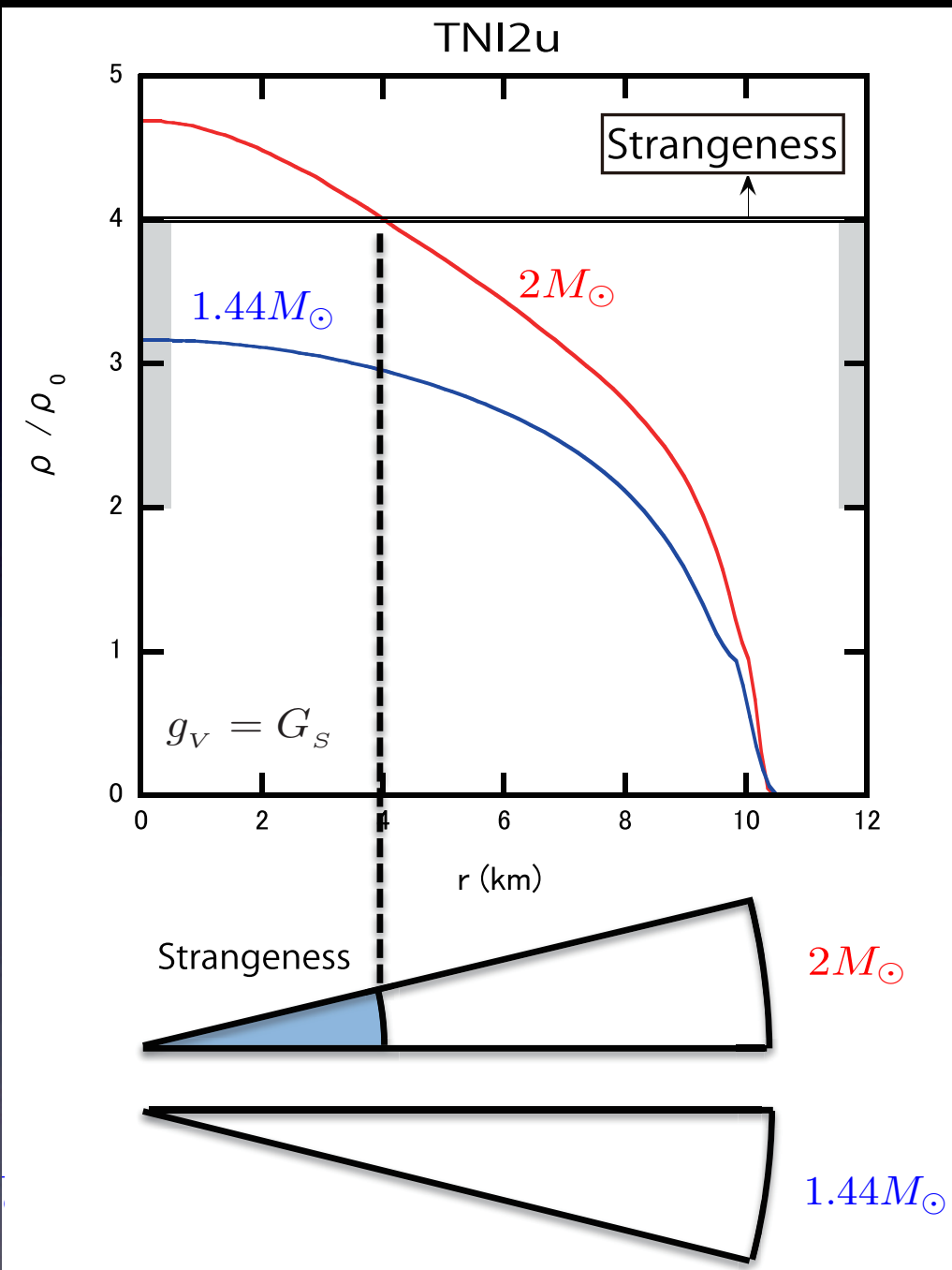


- The emergence of strangeness softens EOS
- Due to the interpolation, the sound velocity increases rapidly in the crossover region

Results (4): Strangeness Core

10/16

$$\rho - r \text{ relation } (\bar{\rho}, \Gamma) = (3\rho_0, \rho_0) \quad g_v = G_S$$



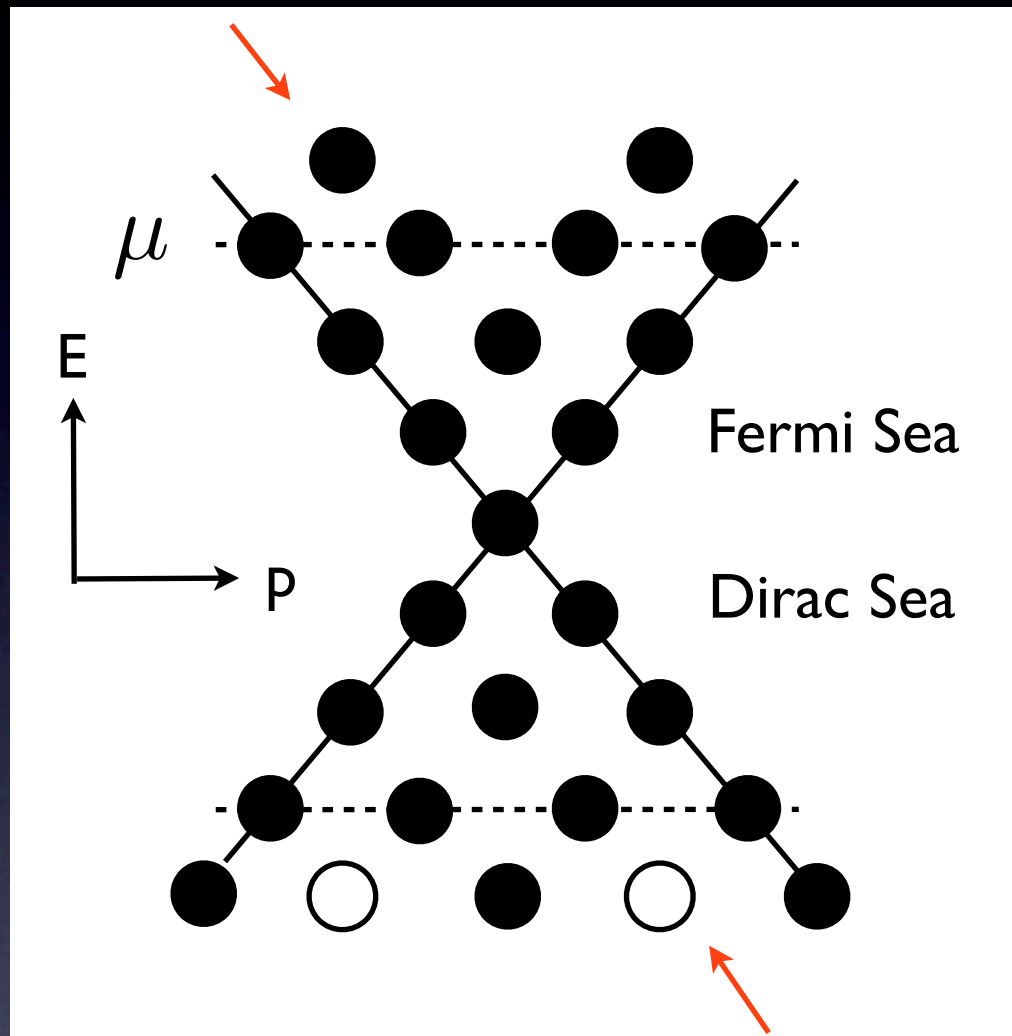
Typical NSs with universal 3-body force do not include strangeness inside themselves

→ possibility of solving cooling problem

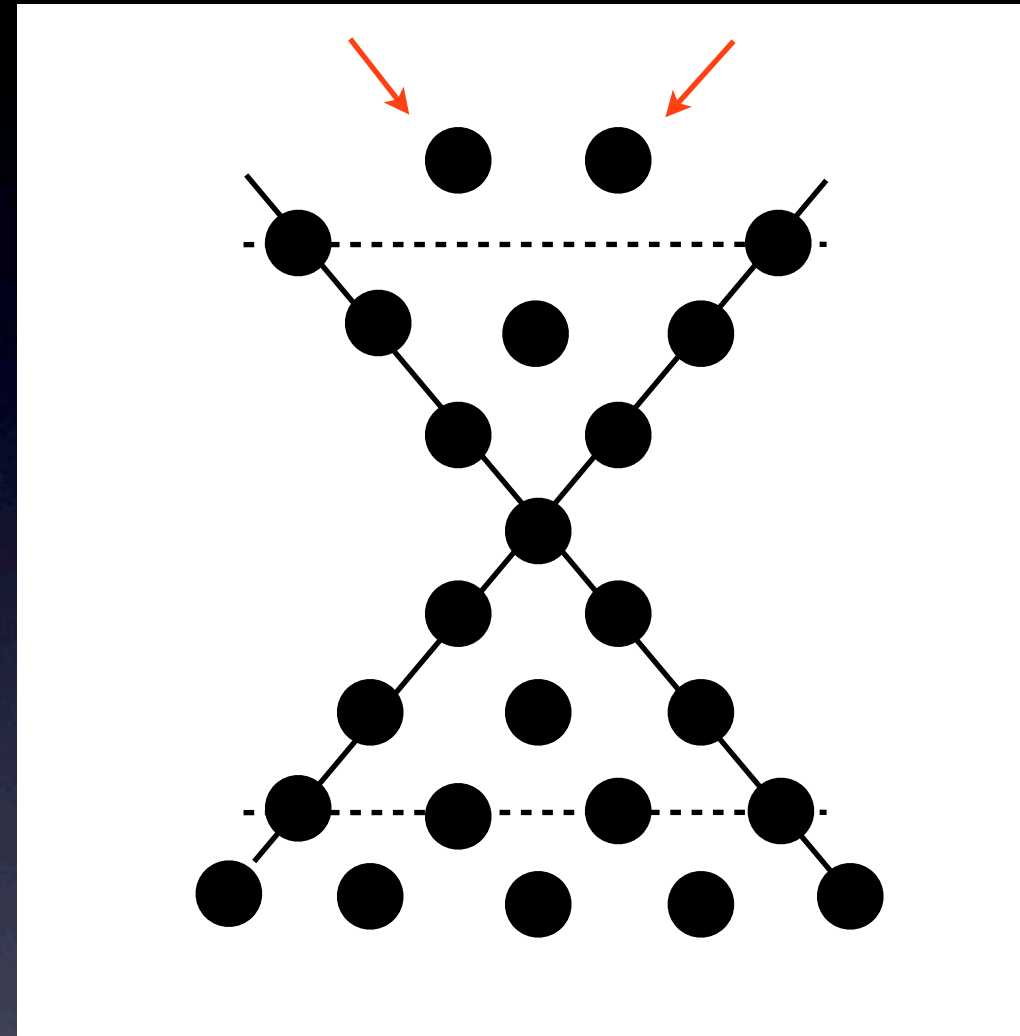
Color Superconductivity (CSC)

11/16

- Chiral Condensate



- Diquark Condensate



Alford

- NJL model

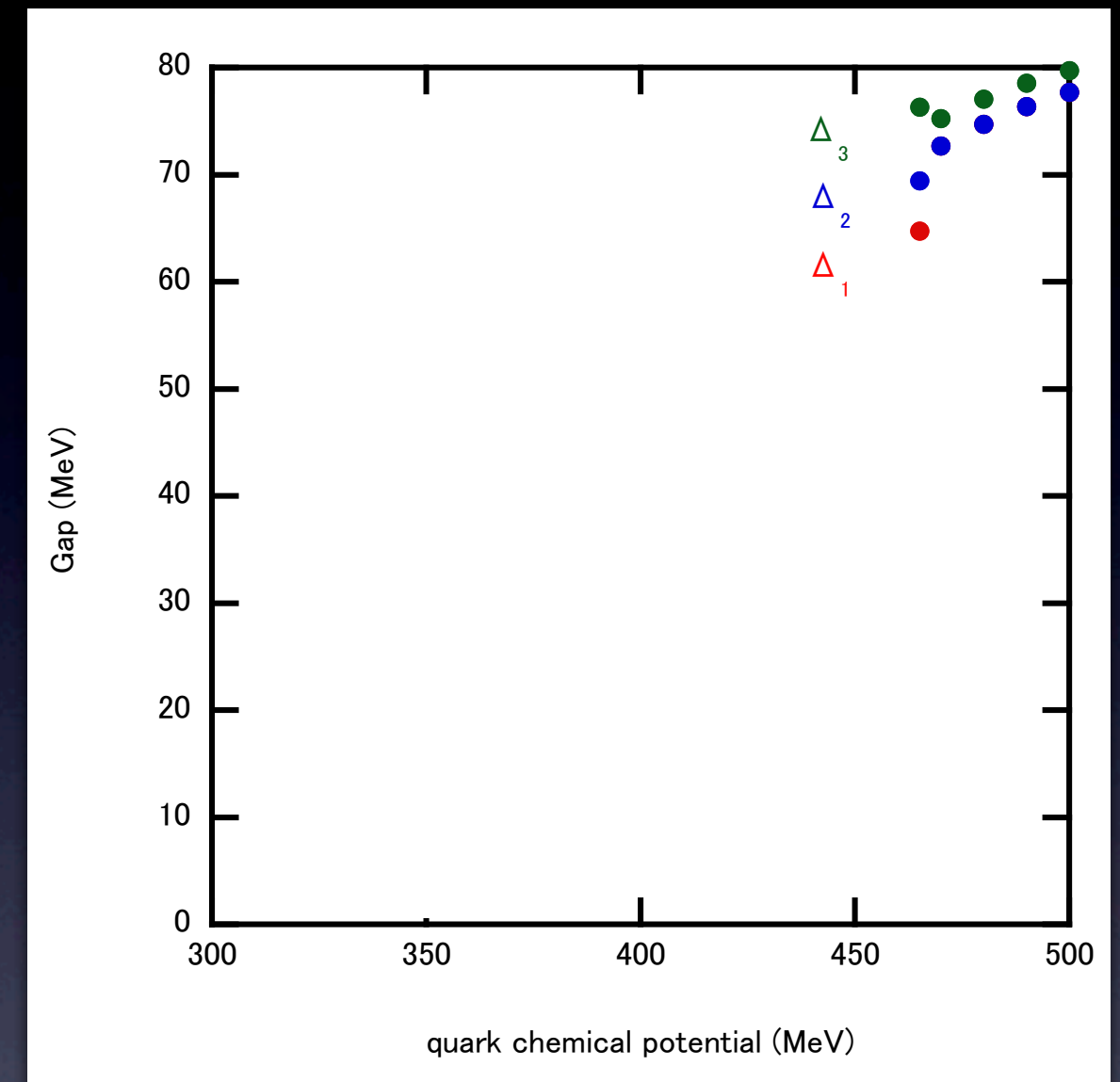
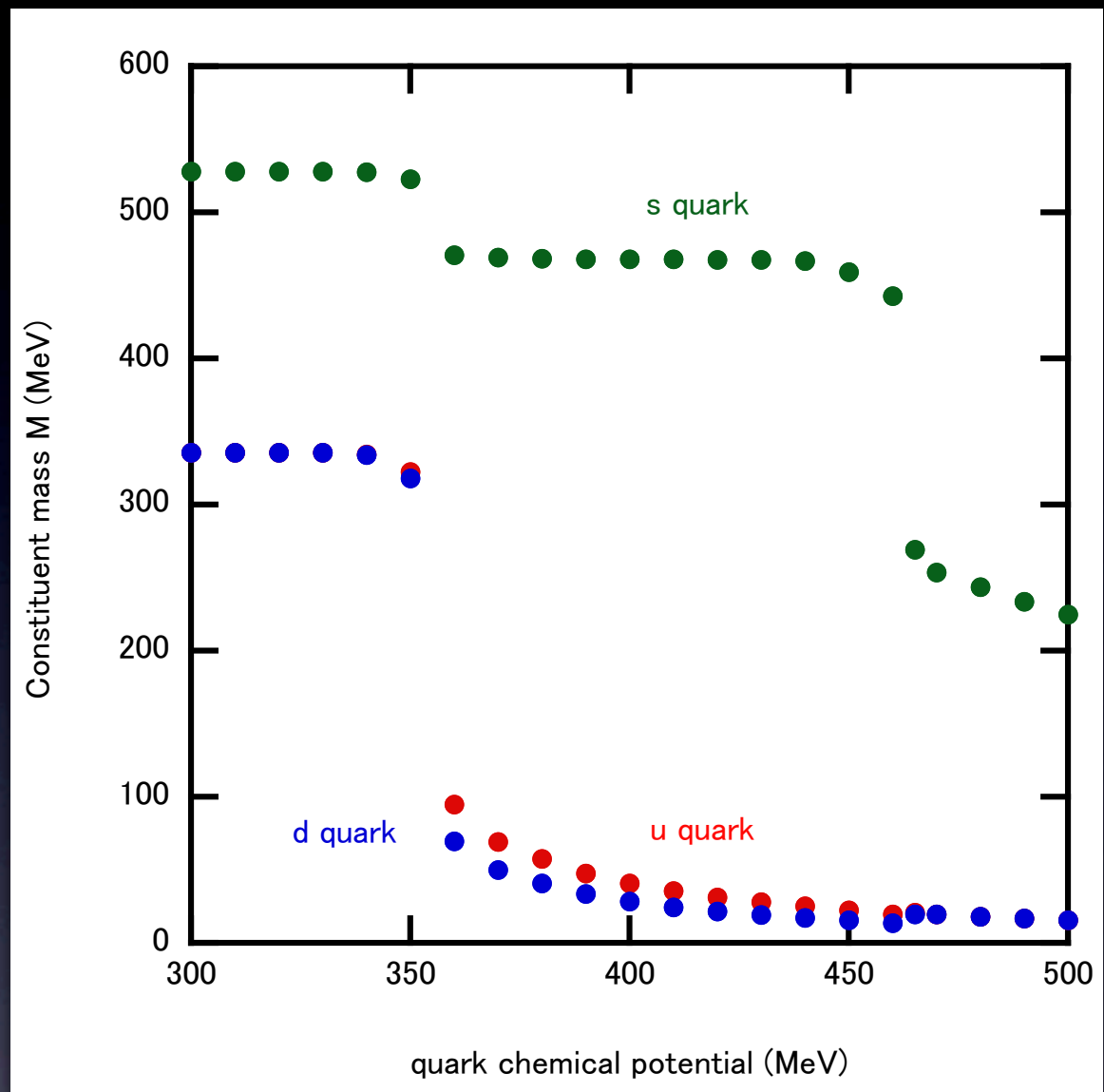
$$L_{\text{CSC}} = L_{\text{NJL}} + \frac{H}{2} \sum_{A=2,5,7} \sum_{A'=2,5,7} (\bar{q} i \gamma_5 \tau_A \lambda_{A'} C \bar{q}^T)(q^T C i \gamma_5 \tau_A \lambda_{A'} q) \quad H = \frac{3}{4} G_s$$

(Fierz)

Results (5): Gap parameter

12/16

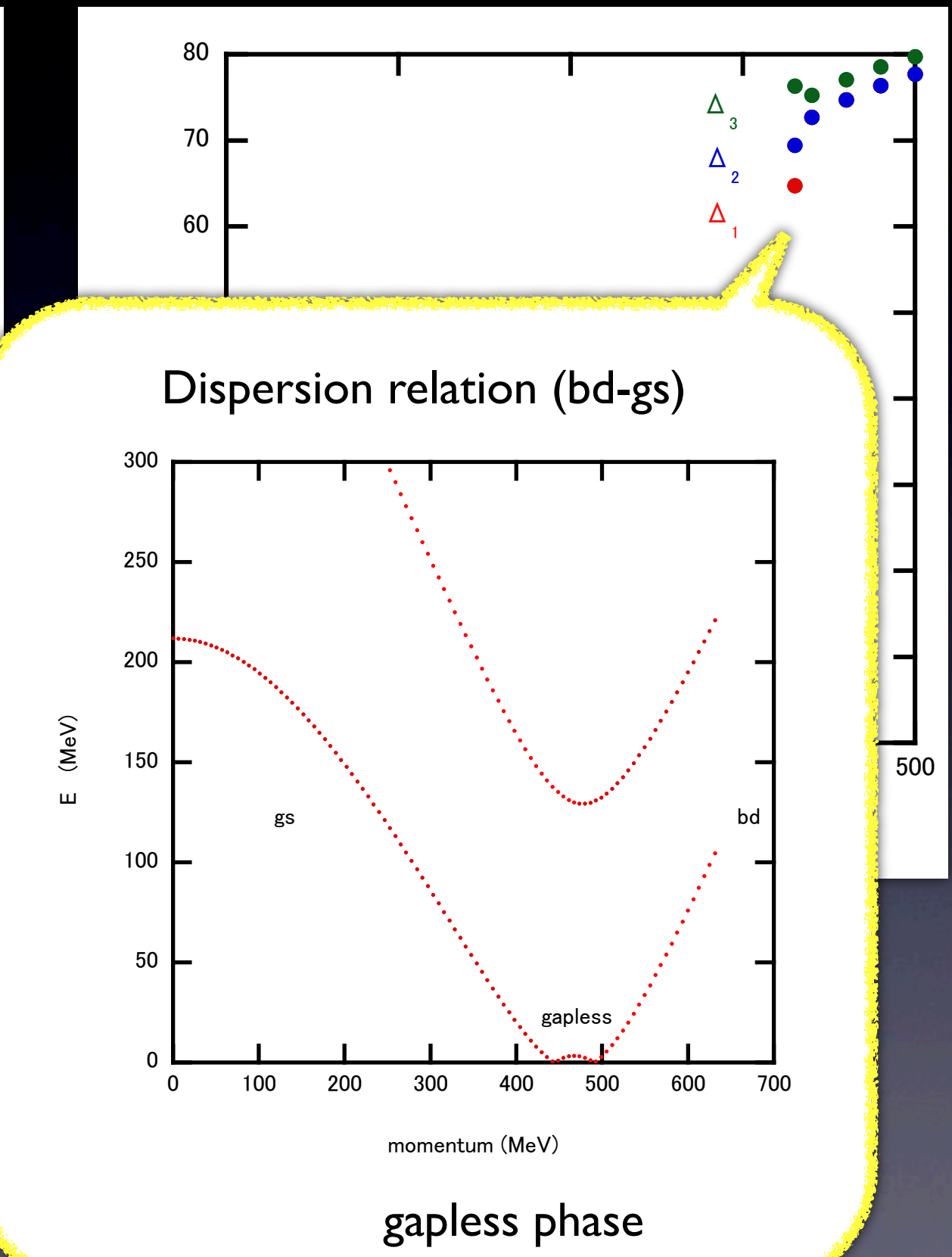
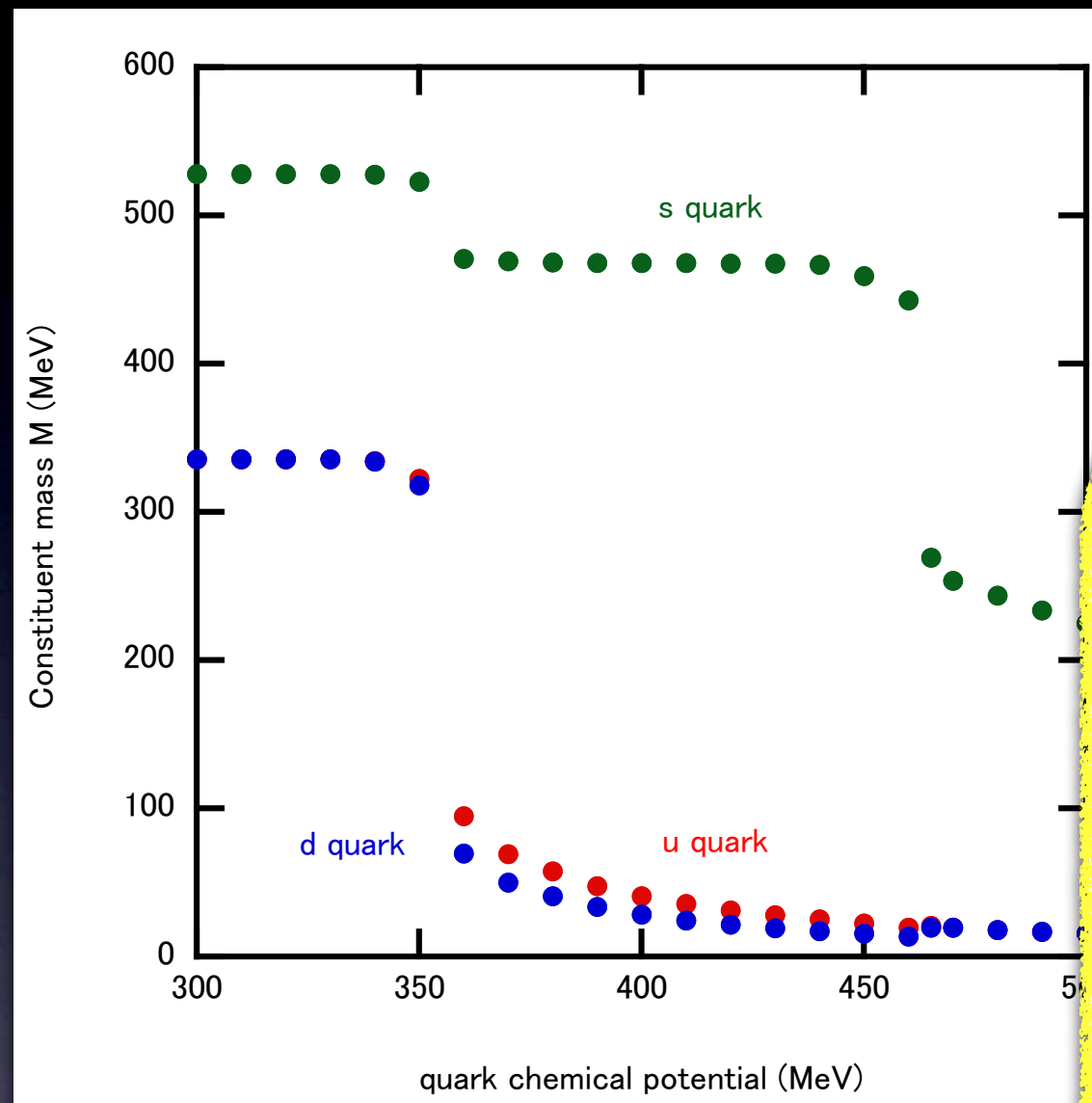
$g_v = 0$



Results (5): Gap parameter

12/16

$$g_v = 0$$



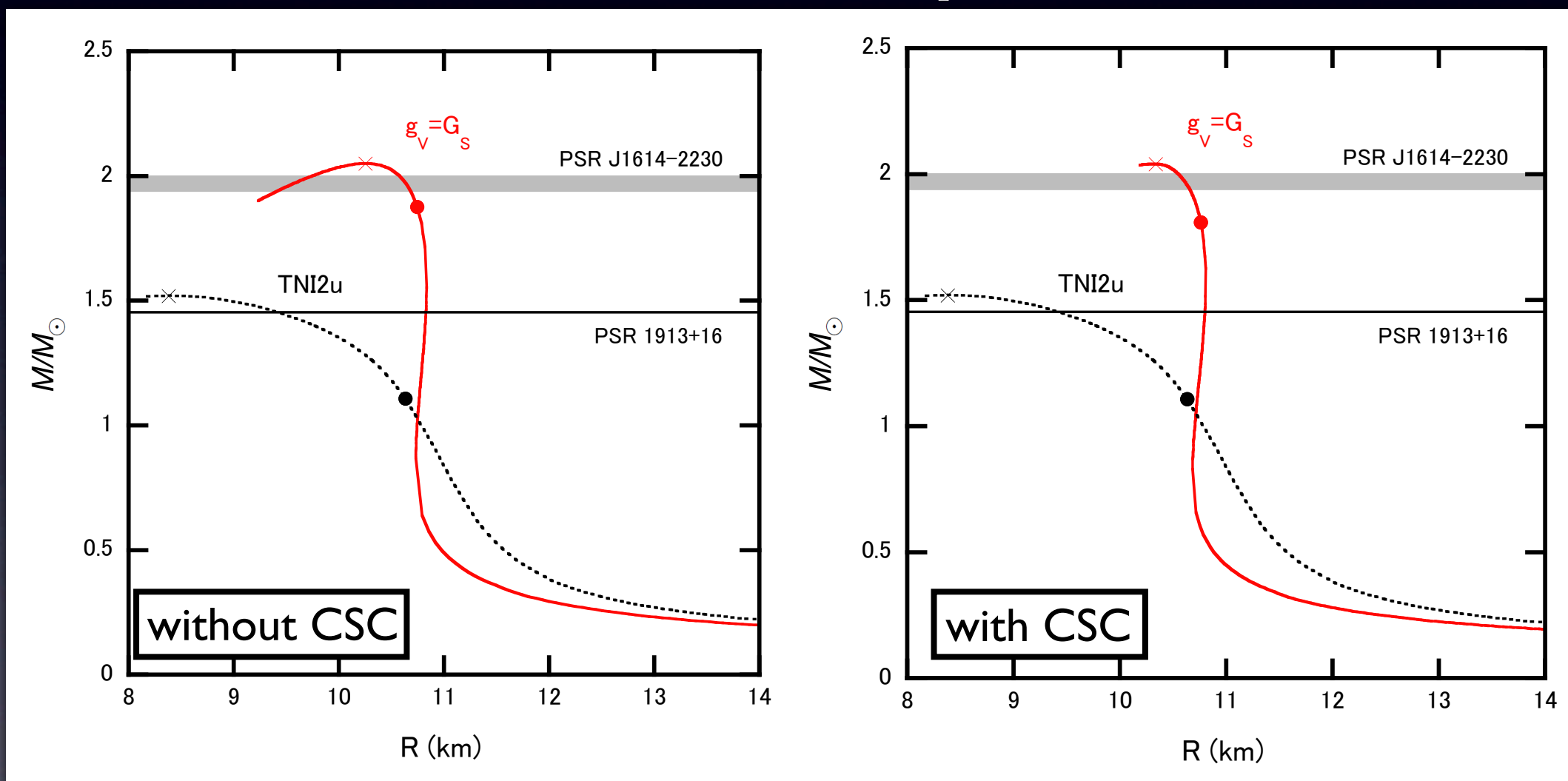
Results (6): Effects of CSC

13/16

Diquark condensation with $J^P = 0^+$

$$L_{\text{CSC}} = L_{\text{NJL}} + \frac{H}{2} \sum_{A=2,5,7} \sum_{A'=2,5,7} (\bar{q} i \gamma_5 \tau_A \lambda_{A'} C \bar{q}^T)(q^T C i \gamma_5 \tau_A \lambda_{A'} q)$$

M-R relation $(\bar{\rho}, \Gamma) = (3\rho_0, \rho_0)$ $g_v = G_S$ $H = \frac{3}{4}G_s$



- CSC softens EOS, but the effects of CSC is very small

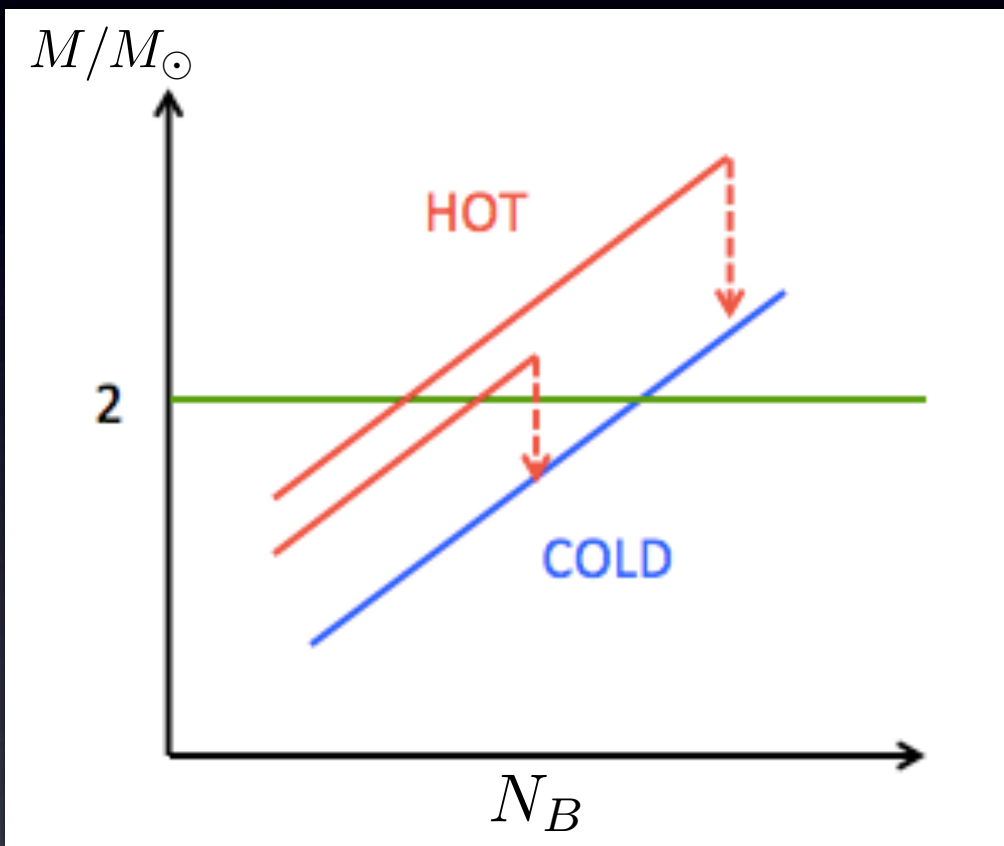
Proto-NS with 2 solar mass puzzle

14/16

At the birth stage, NSs are composed of so-called supernova matter.

- constant lepton fraction
- constant entropy per baryon

$$Y_l = 0.3 - 0.4$$
$$s = 1 - 1.5$$



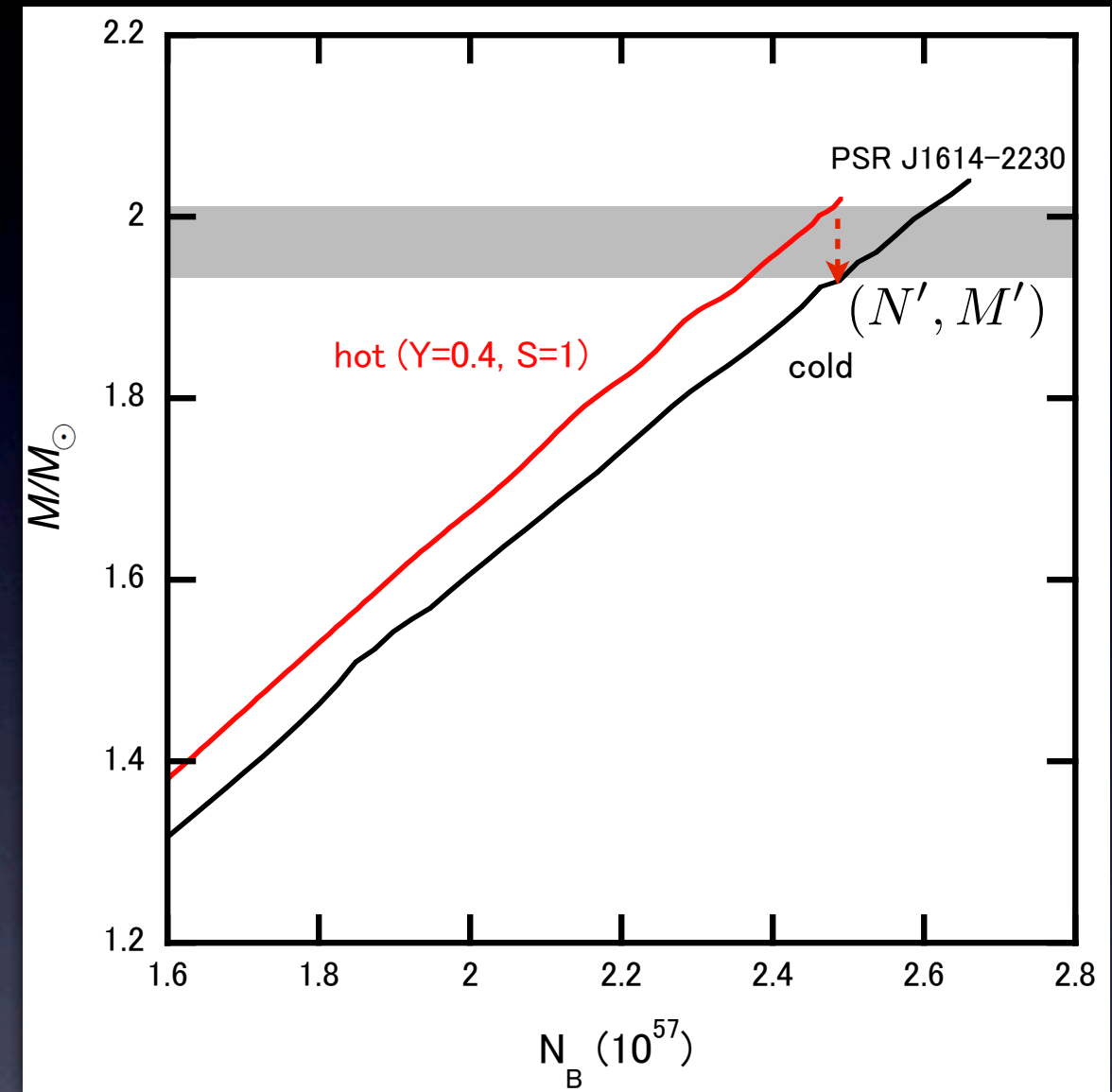
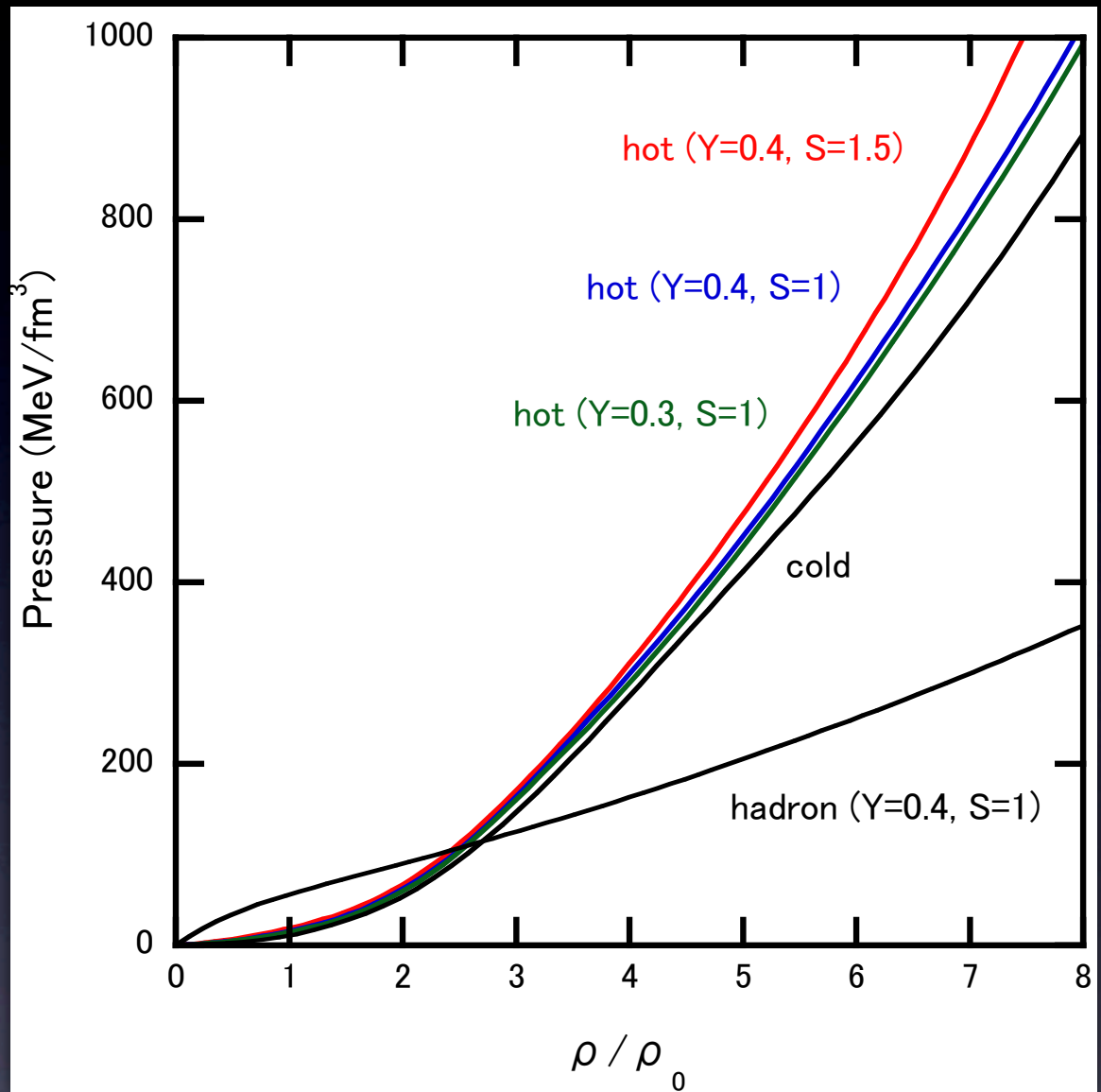
Finite temperature extension of our model

$$P = f_-(\rho) \times p_H(\rho, T)|_{Y_l, s} + f_+(\rho) \times p_Q(\rho, T)|_{Y_l, s}$$

Results (7): Finite T

15/16

$$g_v = G_s \quad (\bar{\rho}, \Gamma) = (3\rho_0, \rho_0)$$



$$N' = 2.49 \times 10^{57}$$

$$M' = 1.92M_\odot < 1.97M_\odot$$

→ neutron star merger ?

Summary

- (1) Crossover occurs at relatively low densities
- (2) Quarks are strongly interacting at and above the crossover region

Interpolated EOS can become stiffer due to the presence of quark matter



Observation of very massive neutron star cannot exclude the existence of the quark matter core



Conventional belief

* Other Characteristics:

Interpolated EOS with the repulsive 3-body force among nucleons and hyperons have a impact on the cooling problem of neutron star with hyperon core

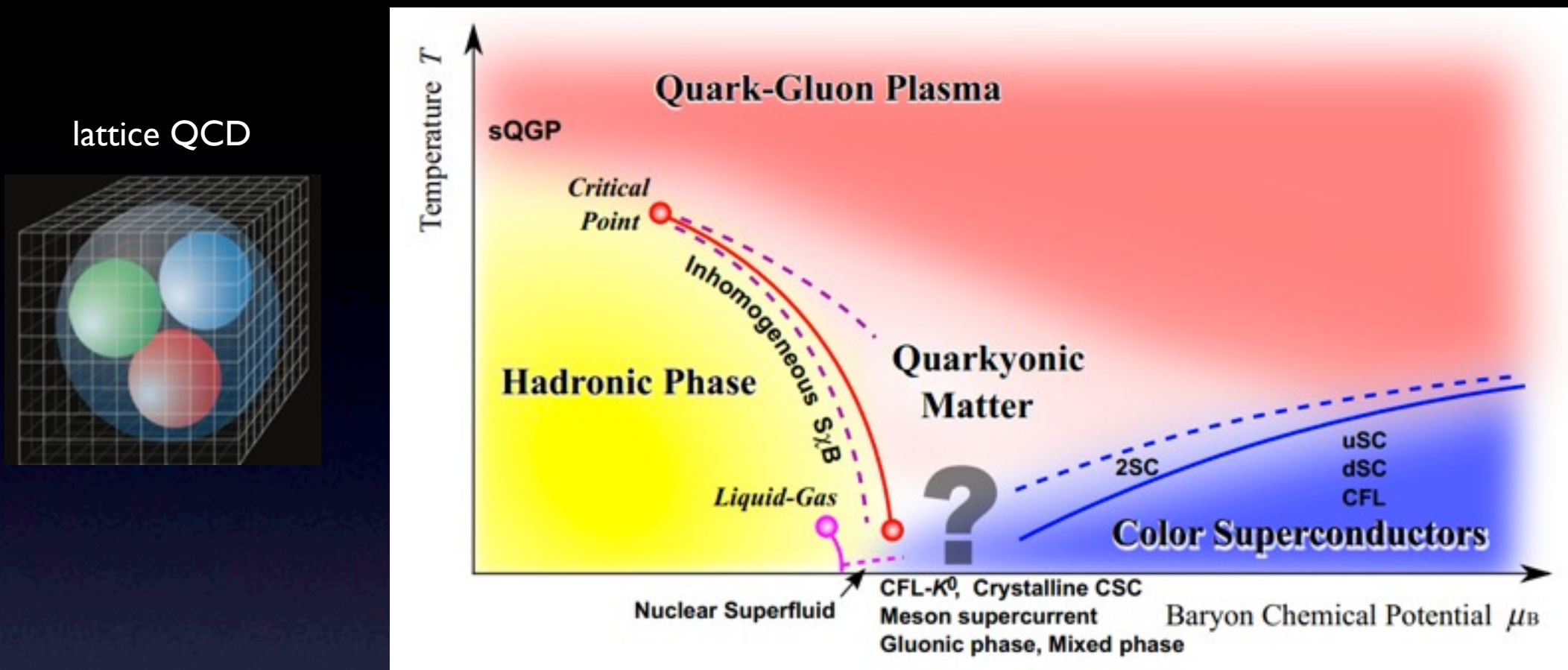
* Perspective

1. Finite temperature extension of the present model (proto-neutron star)
2. Constraints on the EOS from other observables such as neutron star radius and cooling

Back Up Slide

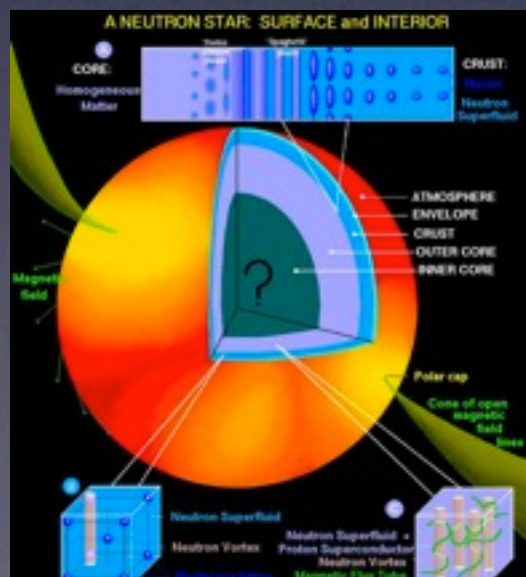
Introduction: QCD Phase Diagram

1/16



Observation

Mass of Neutron stars (NSs)



Theory

Equation of state(EOS):

$$P = f(\varepsilon)$$

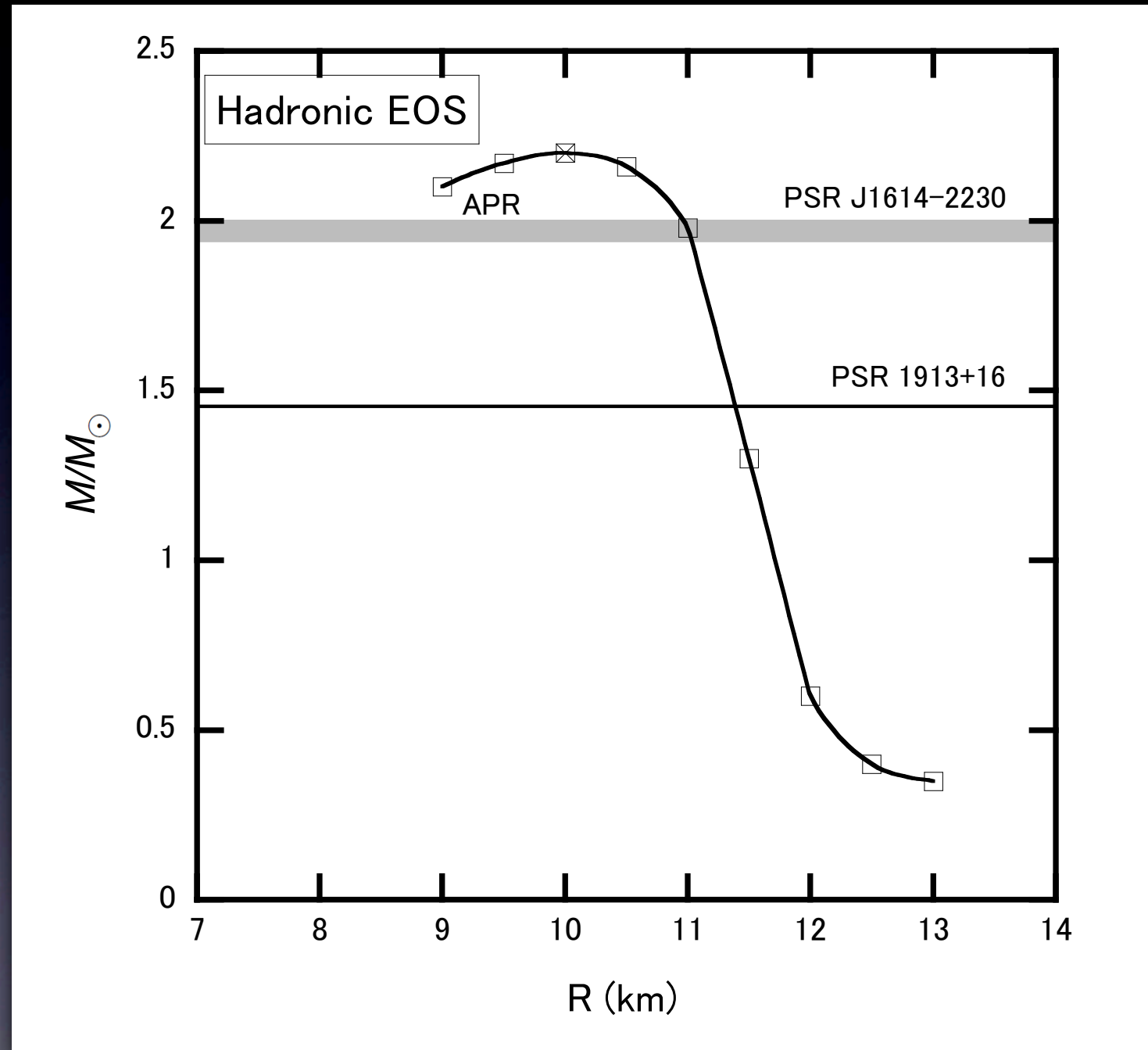
←
constraints
→

Tolman-Oppenheimer-Volkov equation (TOV eq.):

$$\begin{cases} \frac{dP}{dr} = - \left(M + 4\pi P r^3 \right) (\varepsilon + P) \left(\frac{r^2}{G} - 2Mr \right)^{-1} \\ M = \int 4\pi r^2 \varepsilon(x) dr \end{cases}$$

Introduction: Hadronic EOSs

3/16



	APR
Method	Variational
2NF	AV18
3NF	Yes
Hyperons	No

Akmal et al. (1998)

Crossover at finite temperature

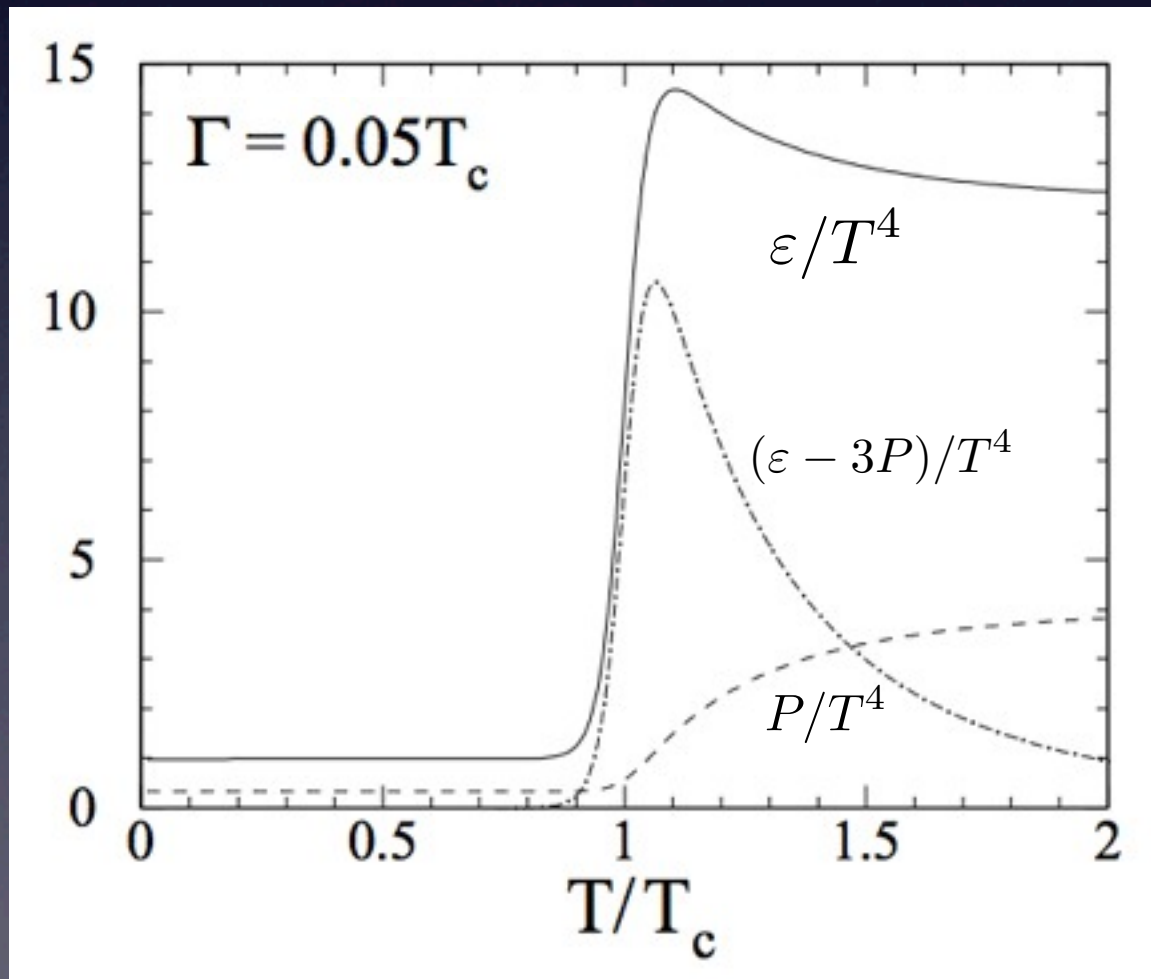
8/29

- Phenomenological Interpolation: $s(T)$

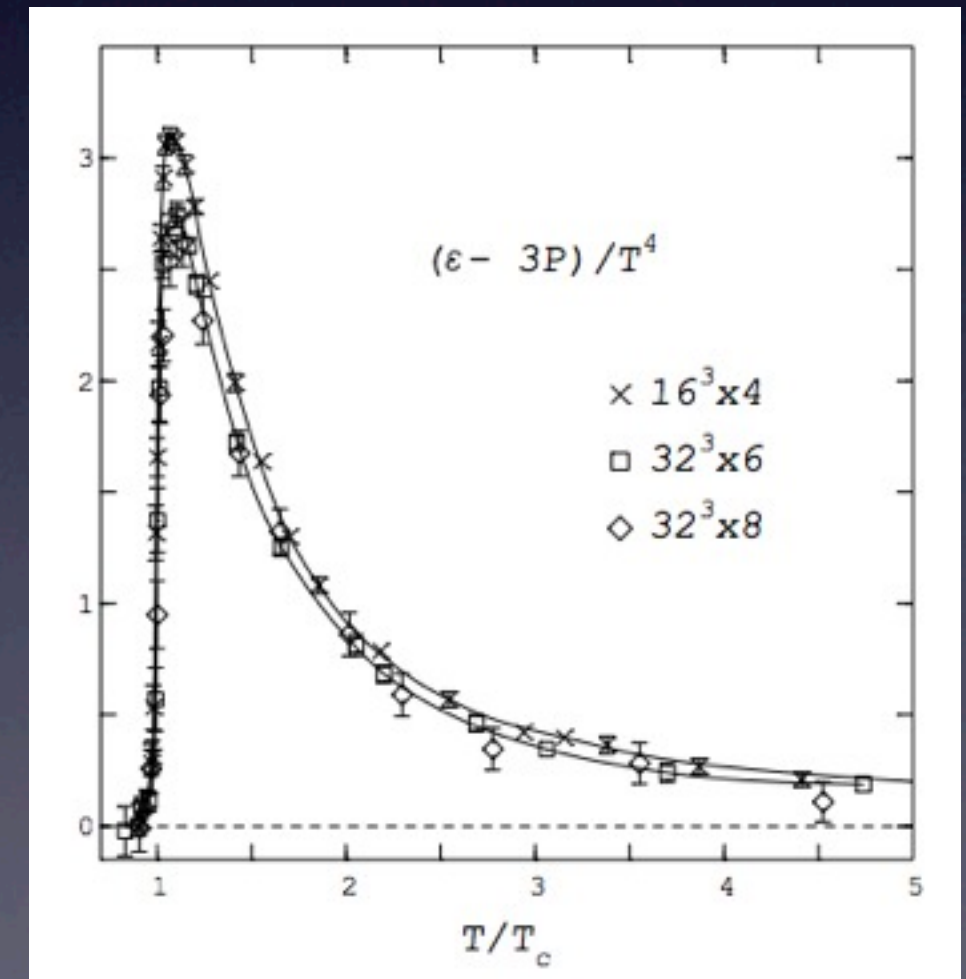
s : entropy density, T : temperature

Asakawa, Hatsuda (1995)

$$\left\{ \begin{array}{l} s(T) = s_h(T)w_h(T) + s_q(T)w_q(T) \\ w_q(T) = \frac{n \left(1 + \tanh \left(\frac{T-T_c}{\Gamma} \right) \right)}{m \left(1 - \tanh \left(\frac{T-T_c}{\Gamma} \right) \right) + n \left(1 + \tanh \left(\frac{T-T_c}{\Gamma} \right) \right)} \end{array} \right.$$



Phenomenological Interpolation



lattice QCD Karsch (1995)

EOS at $\rho \gg \bar{\rho}$

(2+1)-flavor NJL Lagrangian (u,d,s, e^- , μ^-)

$$L_{NJL} = \bar{q}(i\cancel{D} - m)q + \frac{G_s}{2} \sum_{a=0}^8 [(\bar{q}\lambda^a q)^2 + (\bar{q}i\gamma_5\lambda^a q)^2] - \frac{g_v}{2}(\bar{q}\gamma^\mu q)^2 + G_D[\det\bar{q}(1 + \gamma_5)q + \text{h.c.}]$$

$$\downarrow$$

$$\Omega = -\frac{T}{V} \ln Z = \Omega_q(M, \mu^{\text{eff}}) + \Omega_l + G_s \sum \langle \bar{q}_i q_i \rangle^2 + 4G_D \langle \bar{q}_i q_i \rangle \langle \bar{q}_j q_j \rangle \langle \bar{q}_k q_k \rangle - \frac{1}{2} g_v \left(\sum_i \langle q_i^\dagger q_i \rangle \right)^2$$

$$\Omega_q(\mu^{\text{eff}}) = -T \sum_i \sum_l \int \frac{d^3 p}{(2\pi)^3} \text{Tr} \ln \left(\frac{1}{T} S_i^{-1}(i\omega_l, \vec{p}) \right),$$

$$S_i^{-1} = p - \mu^{\text{eff}} \gamma^0 - M_i, \quad p^0 = i\omega_l = (2l + 1)\pi T$$

Gap equations: $\frac{\partial \Omega}{\partial \langle \bar{q}_i q_i \rangle} = 0$

Parameter sets

cutoff (MeV)	$G_s \Lambda^2$	$G_D \Lambda^5$	$m_{u,d}(MeV)$	$m_s(MeV)$
631.4	3.67	9.29	5.5	135.7

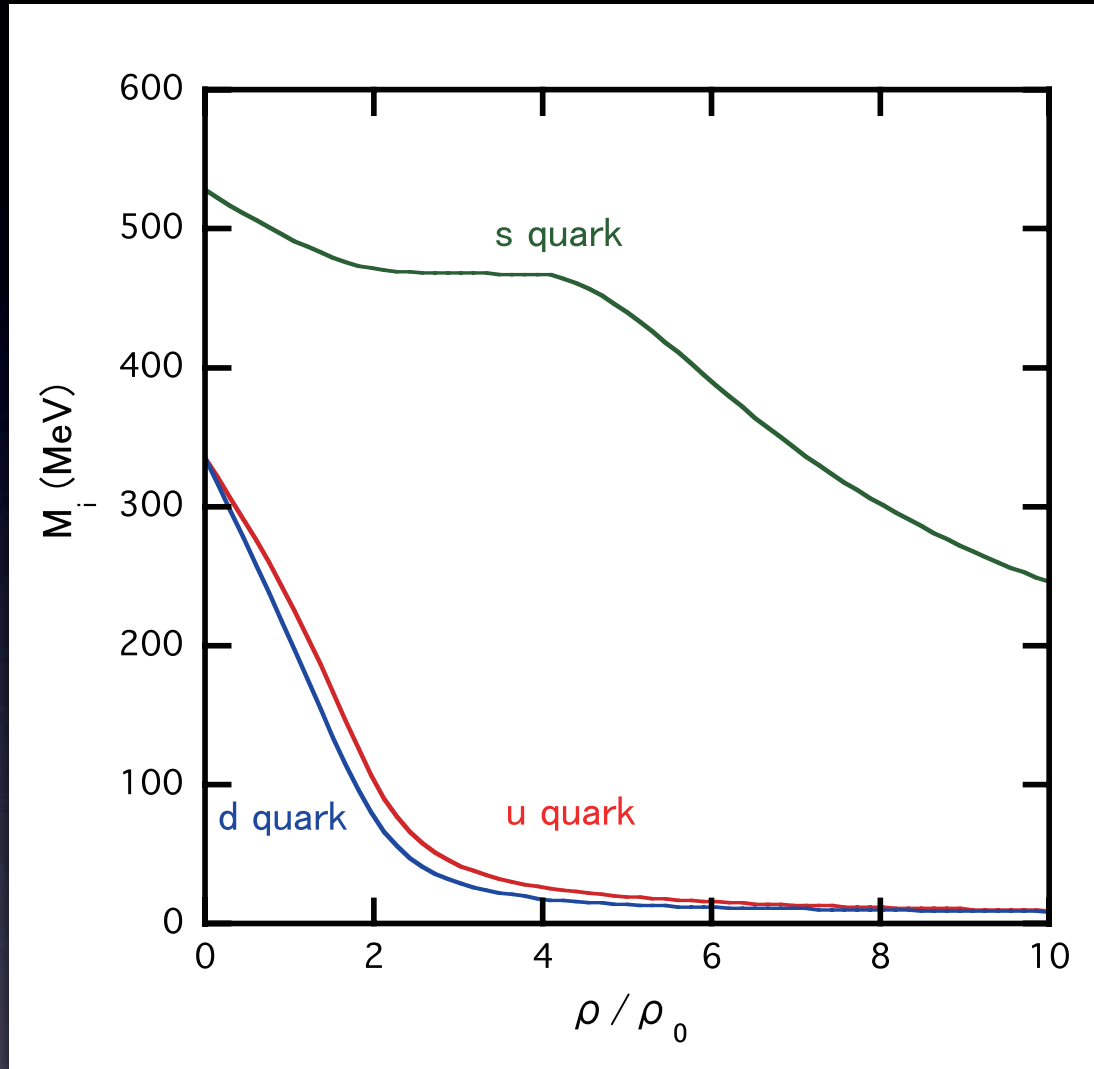
$$0 \leq g_v \leq 1.5G_s$$

(Fierz: $G_v = 0.5G_s$)

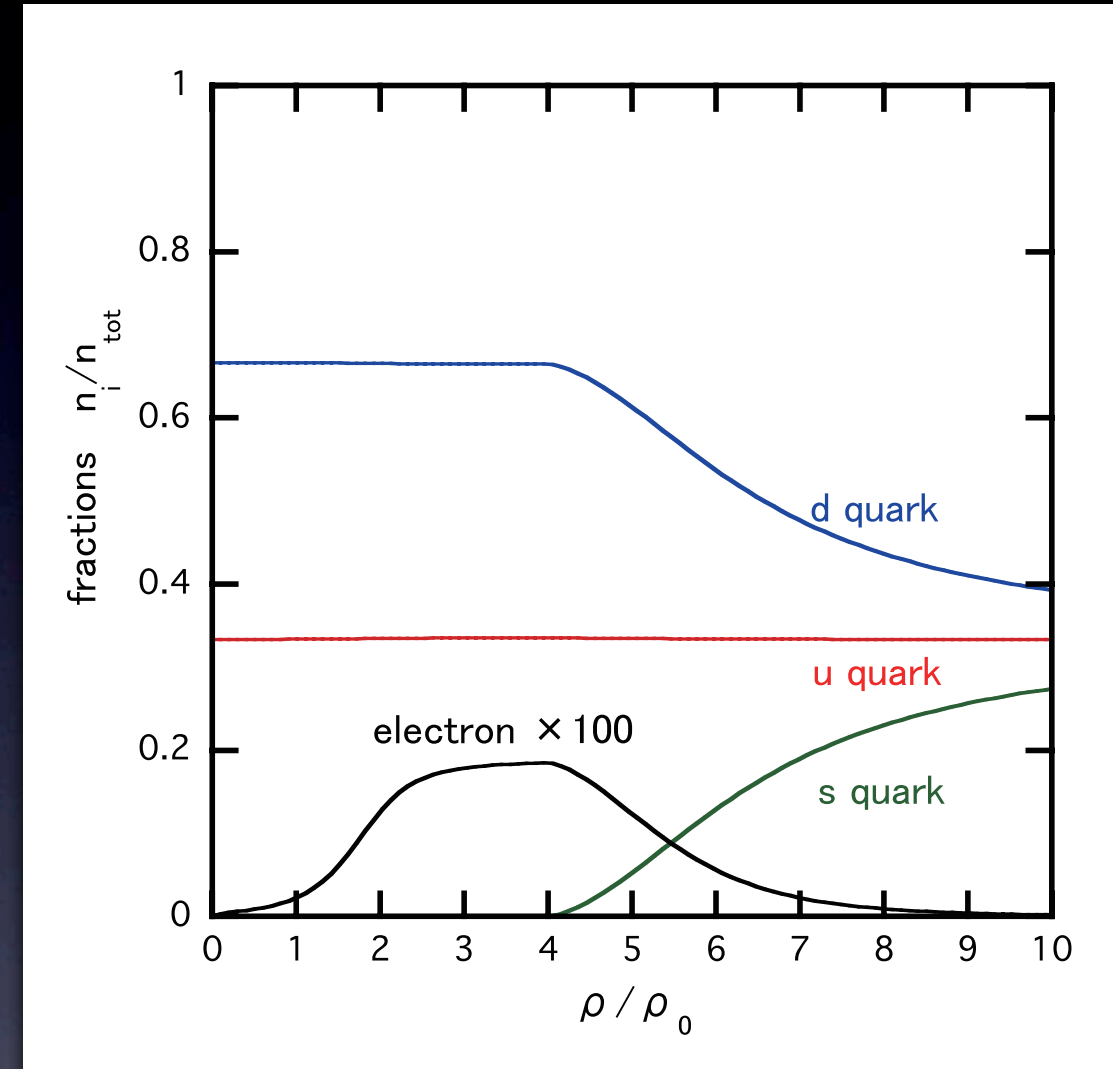
Conditions:

1. beta-equilibrium
2. charge neutrality

Constituent mass



Number fraction

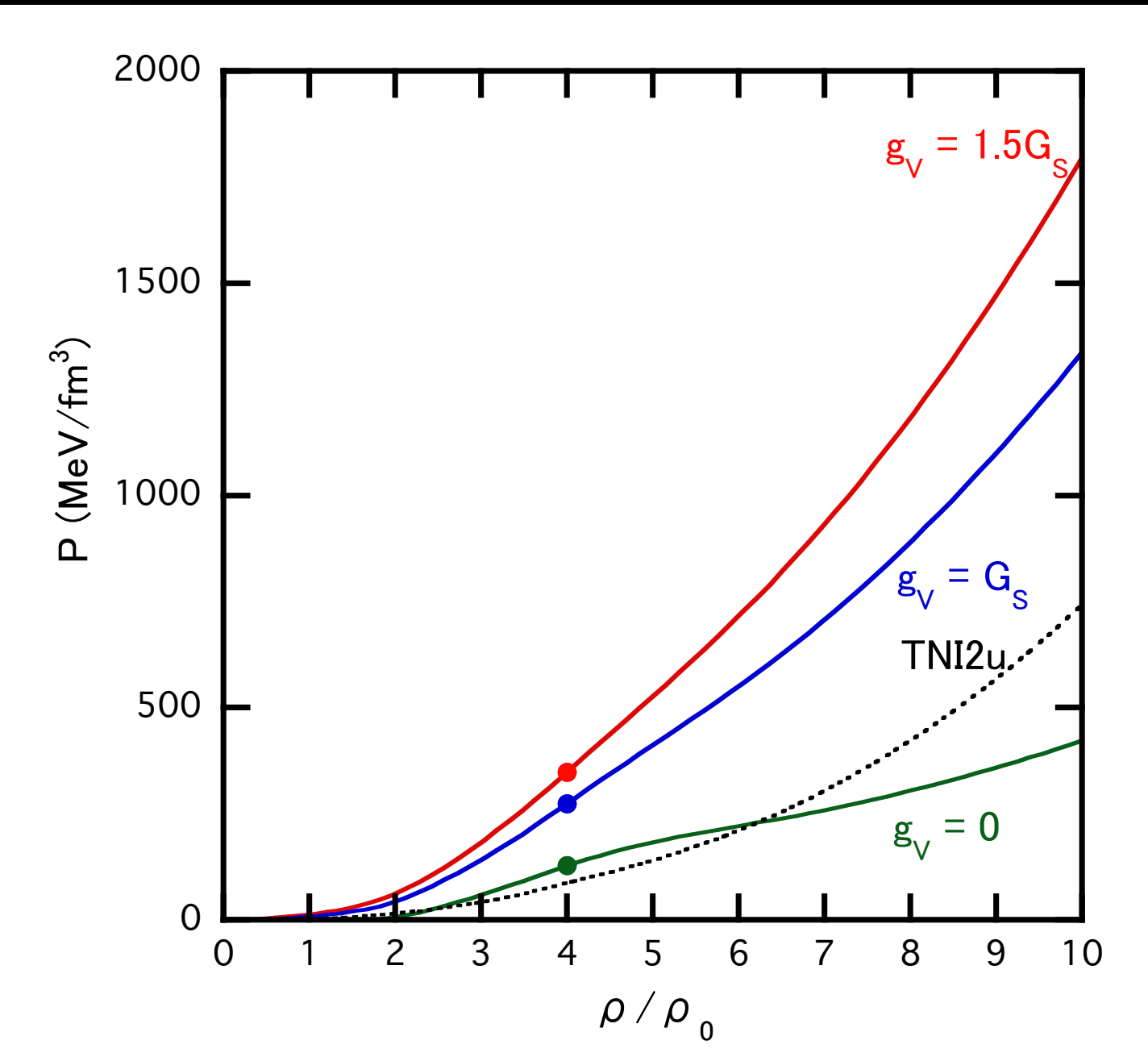


Chiral restoration

- u,d quark : low densities
- s quark : $4 \rho_0$

- s quark starts to appear above $4 \rho_0$
- SU(3) flavor symmetric matter at high densities
- muon does not appear due to
 - s quark
 - charge neutrality
- figures do not depend on the magnitude of vector interaction

Pressure P

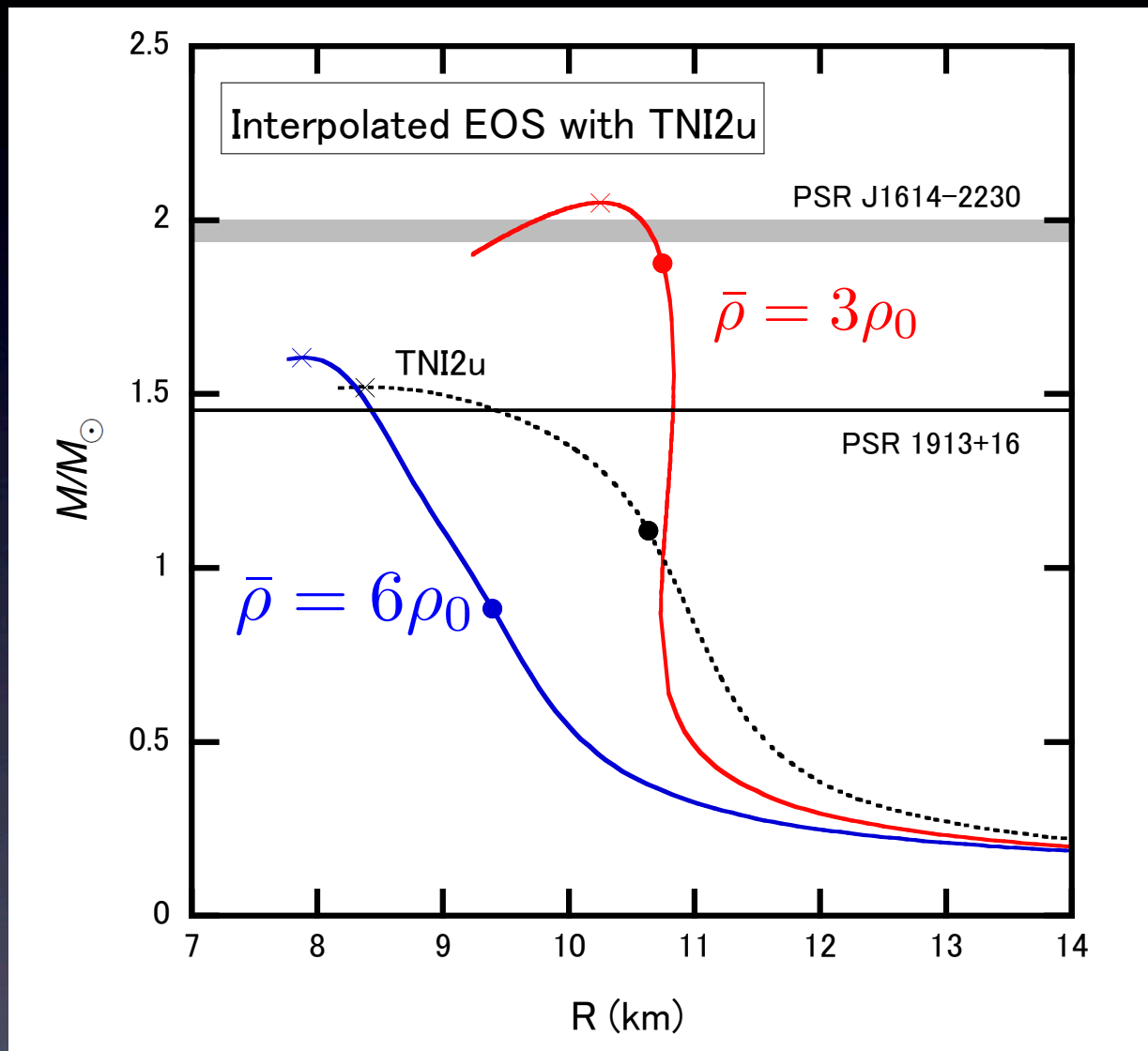


- EOS becomes stiffer as g_V increases due to the universal repulsion

Results (2): Effects of Crossover Density ($\bar{\rho}$)

16/29

M-R relation $\Gamma = \rho_0$ $g_v = G_S$

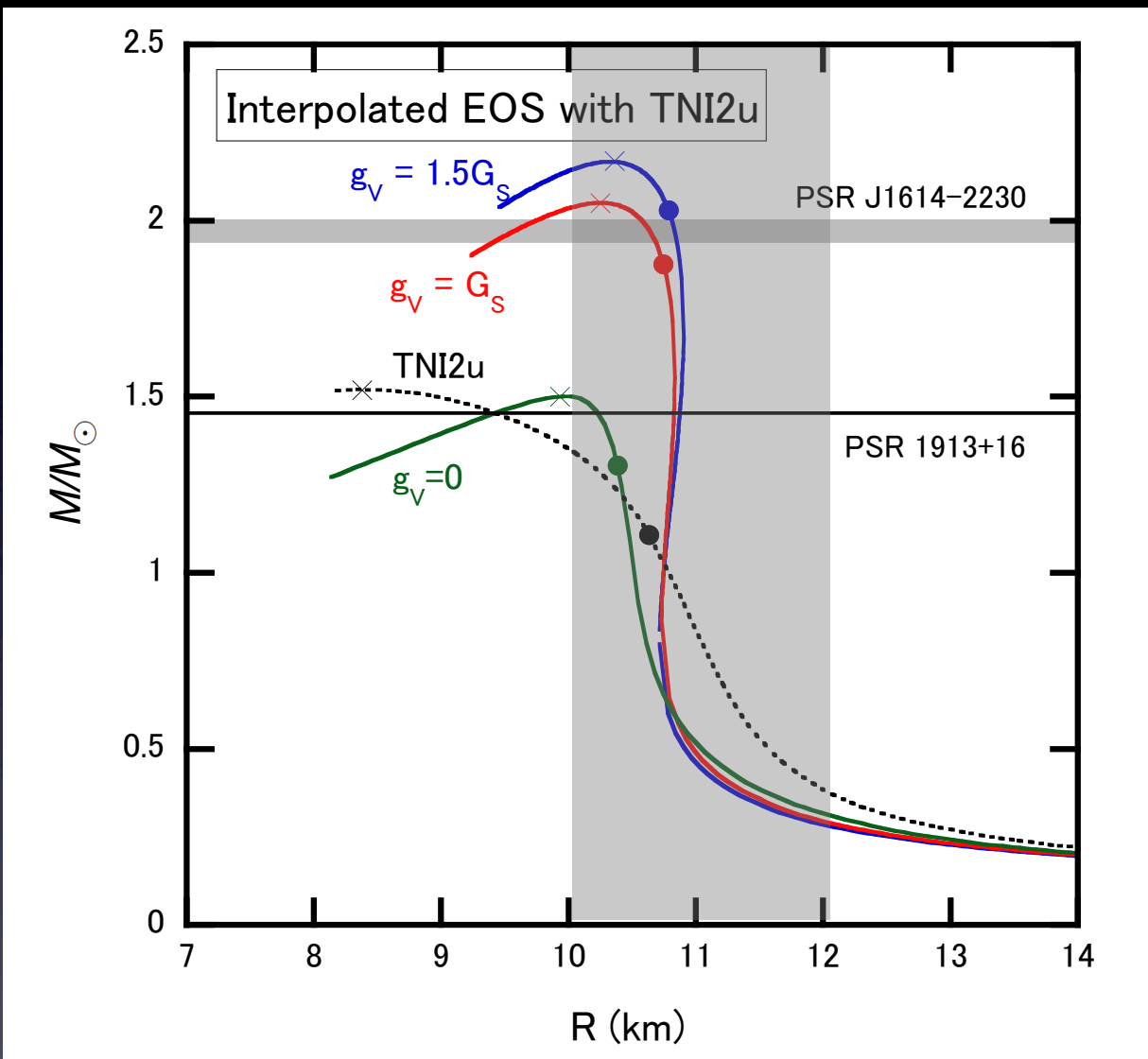


- Crossover occurs at relatively low densities $\rightarrow 2M_\odot$

Results (3): Effects of Vector Int. (g_V)

17/29

M-R relation $(\bar{\rho}, \Gamma) = (3\rho_0, \rho_0)$



- The maximum mass exceeds $2M_\odot$ only if the vector type repulsion is as strong as the scalar interaction
- Radius: about 11 km

Another Interpolation

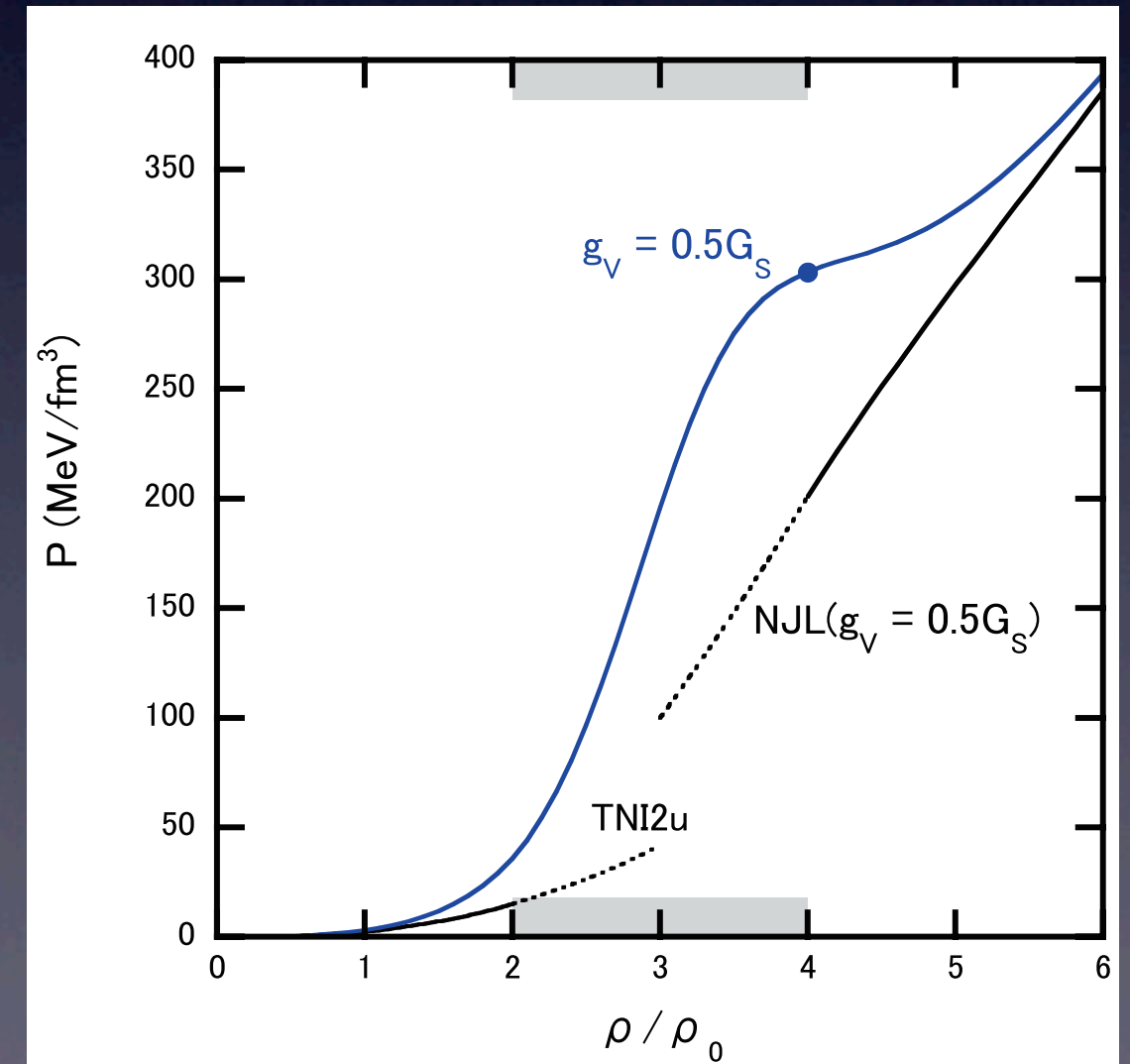
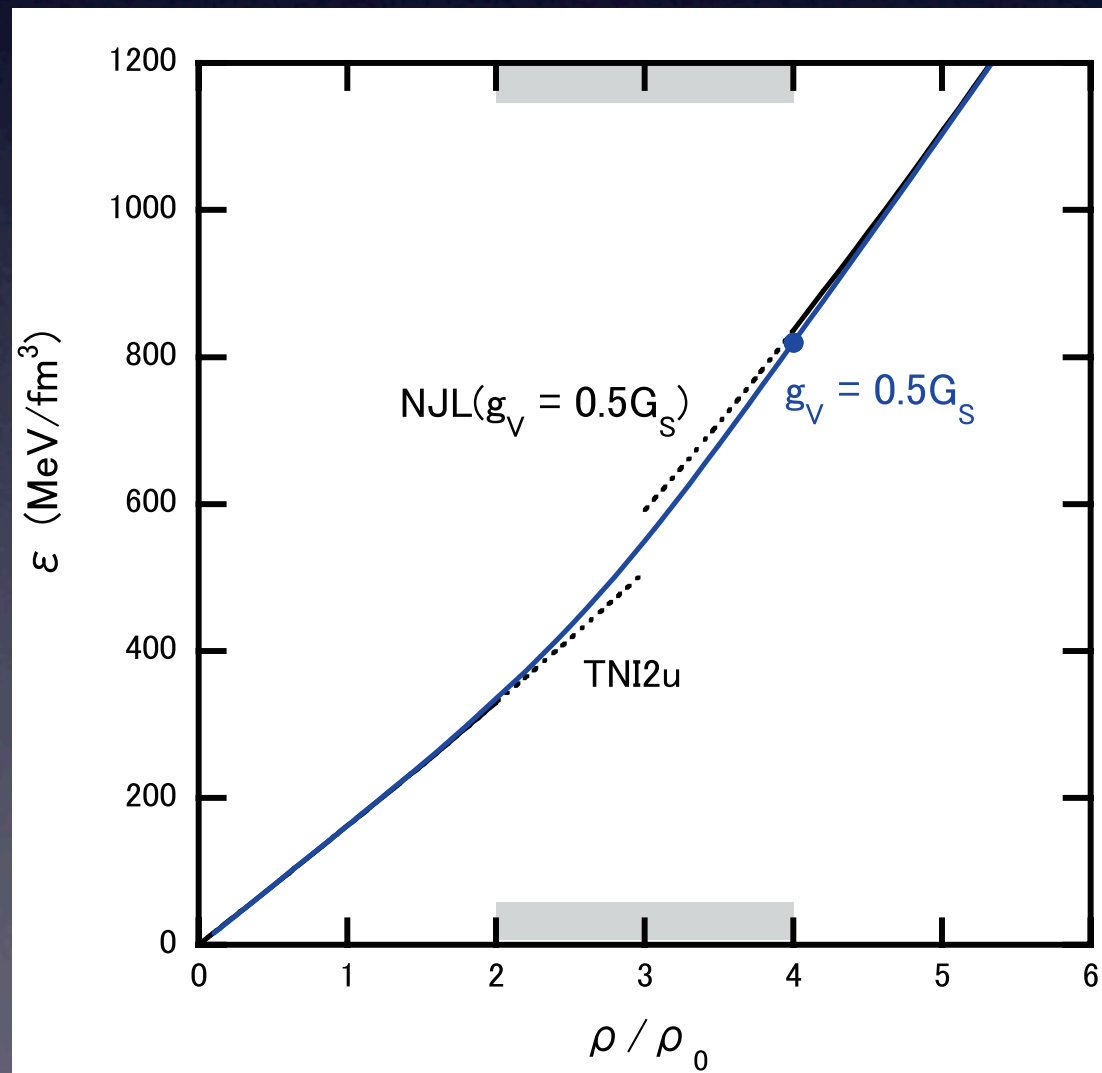
21/29

Phenomenological interpolation: $\varepsilon(\rho)$

$$\left[\begin{array}{l} \varepsilon = \varepsilon_H \times f_- + \varepsilon_Q \times f_+ \quad f_{\pm} = \frac{1 \pm \tanh(\frac{\rho - \bar{\rho}}{\Gamma})}{2} \\ P = \rho^2 \frac{\partial(\varepsilon/\rho)}{\rho} \end{array} \right]$$

H-EOS:TNI2u, Q-EOS: NJL

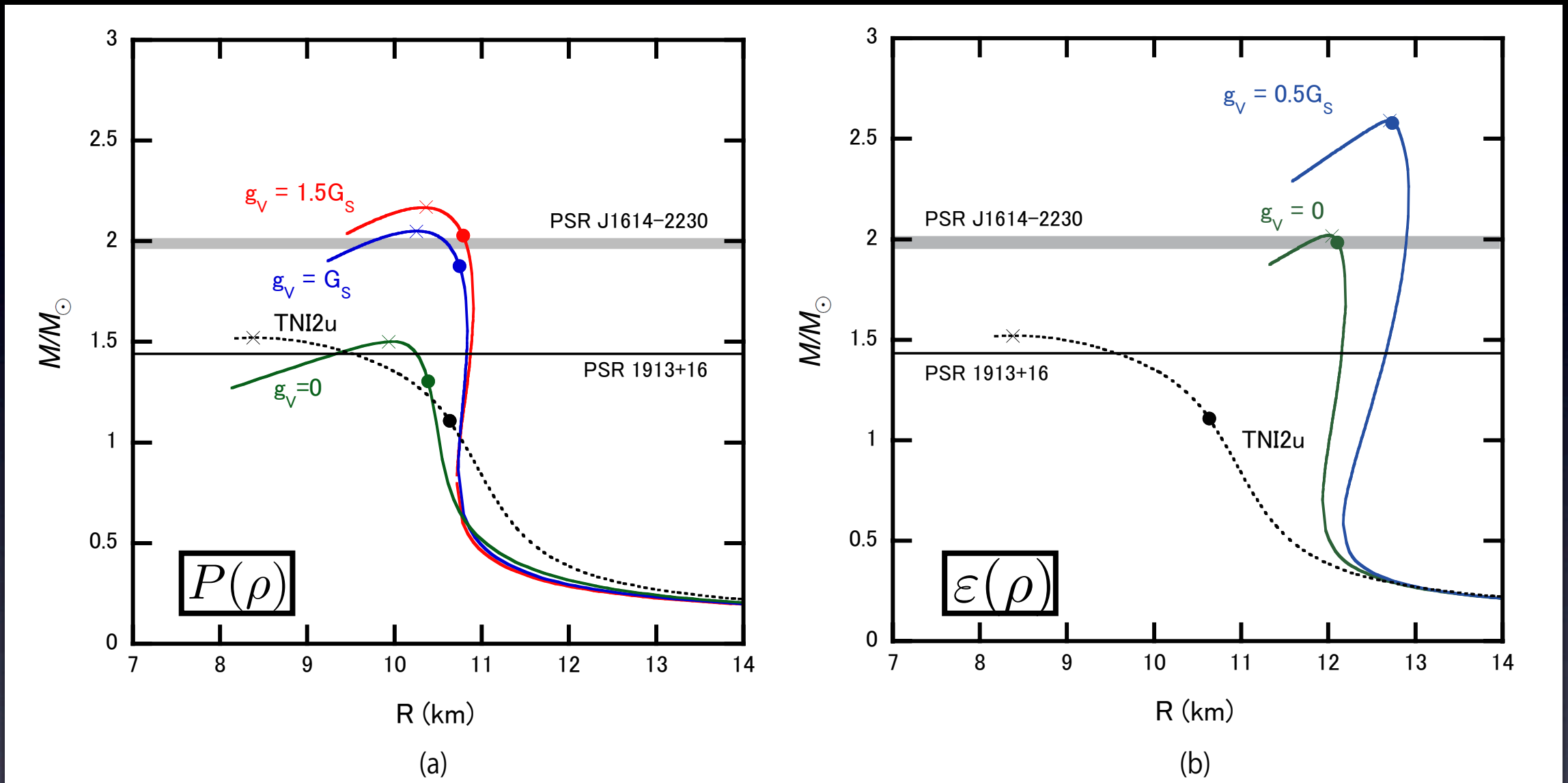
$$g_v = 0.5G_s \quad (\bar{\rho}, \Gamma) = (3\rho_0, \rho_0)$$



Results (7): Effects of Method

22/29

M-R relation $(\bar{\rho}, \Gamma) = (3\rho_0, \rho_0)$



- The ϵ -interpolation makes EOS stiff more drastically than the P -interpolation.
- Even for $(g_v, \bar{\rho}) = (0, 3\rho_0)$, the maximum mass can exceed $1.97 M_\odot$.

CSC Lagrangian

$$L_{\text{CSC}} = L_{\text{NJL}} + \frac{H}{2} \sum_{A=2,5,7} \sum_{A'=2,5,7} (\bar{q} i \gamma_5 \tau_A \lambda_{A'} C \bar{q}^T) (q^T C i \gamma_5 \tau_A \lambda_{A'} q) \quad H = \frac{3}{4} G_s$$

by Fierz

$$q^C = C \bar{q}^T \quad \Psi = \frac{1}{\sqrt{2}} \begin{pmatrix} q \\ q^C \end{pmatrix}$$

$$\Delta_1 = -H s_{55}, \quad \Delta_2 = -H s_{77}, \quad \Delta_3 = -H s_{22}$$

$$\Omega(T, \mu_{u,d,s}) = -\frac{T}{2} \sum_{\ell} \int \frac{d^3 p}{(2\pi)^3} \text{Tr} \ln \left(\frac{S^{-1}(i\omega_{\ell}, \mathbf{p})}{T} \right) + G_s \sum_i \sigma_i^2$$

$$+ 4G_D \sigma_u \sigma_d \sigma_s - \frac{1}{2} g_V \left(\sum_i n_i \right)^2 + \frac{1}{2H} \sum_{\text{color}} |\Delta_c|^2$$

$$S^{-1} = \begin{pmatrix} S_{0+}^{-1} & \Phi^- \\ \Phi^+ & S_{0-}^{-1} \end{pmatrix} \quad (\Phi^-)_{ab}^{\alpha\beta} = - \sum_{\text{color}} \varepsilon^{\alpha\beta c} \varepsilon_{abc} \Delta_c \gamma_5, \quad \Phi^+ = \gamma^0 (\Phi^-)^\dagger \gamma^0$$

$$S_{0\pm}^{-1} = p - M \pm \tilde{\mu} \gamma^0$$

$$\tilde{\mu} = \mu - \frac{1}{2} \mu_3 - \frac{1}{2\sqrt{3}} \mu_8$$

CSC Lagrangian (2)

Buballa (2004)

$$p = \frac{1}{4\pi^2} \sum_{i=1,36} \int_0^\Lambda dpp^2 \left(|\varepsilon_i| + 2T \ln \left(1 + e^{-|\varepsilon_i/T|} \right) \right) - G_s \sum_i \sigma_i^2$$

$$-4G_D \sigma_u \sigma_d \sigma_s + \frac{1}{2} g_V \left(\sum_i n_i^2 \right)^2 - \frac{1}{2H} \sum_{\text{color}} |\Delta_c|^2$$

Gap equations: $\frac{\partial p}{\partial \sigma_i} = \frac{\partial p}{\partial \Delta_i} = \frac{\partial p}{\partial \mu_i} = 0$

$$\begin{pmatrix} -\mu_d^r + M_d & p & 0 & -\Delta_3 \\ p & -\mu_d^r - M_d & \Delta_3 & 0 \\ 0 & \Delta_3 & \mu_u^g + M_u & p \\ -\Delta_3 & 0 & p & \mu_u^g - M_u \end{pmatrix} \begin{pmatrix} \mu_d^r - M_d & p & 0 & -\Delta_3 \\ p & \mu_d^r + M_d & \Delta_3 & 0 \\ 0 & \Delta_3 & -\mu_u^g - M_u & p \\ -\Delta_3 & 0 & p & -\mu_u^g + M_u \end{pmatrix} \begin{pmatrix} -\mu_s^r + M_s & p & 0 & -\Delta_2 \\ p & -\mu_s^r - M_s & \Delta_2 & 0 \\ 0 & \Delta_2 & \mu_u^b + M_u & p \\ -\Delta_2 & 0 & p & \mu_u^b - M_u \end{pmatrix}$$

$$\begin{pmatrix} \mu_s^r - M_s & p & 0 & -\Delta_2 \\ p & \mu_s^r + M_s & \Delta_2 & 0 \\ 0 & \Delta_2 & -\mu_u^b - M_u & p \\ -\Delta_2 & 0 & p & -\mu_u^b + M_u \end{pmatrix} \begin{pmatrix} -\mu_s^g + M_s & p & 0 & -\Delta_1 \\ p & -\mu_s^g - M_s & \Delta_1 & 0 \\ 0 & \Delta_1 & \mu_d^b + M_u & p \\ -\Delta_1 & 0 & p & \mu_d^b - M_d \end{pmatrix} \begin{pmatrix} \mu_s^g - M_s & p & 0 & -\Delta_1 \\ p & \mu_s^g + M_s & \Delta_1 & 0 \\ 0 & \Delta_1 & -\mu_d^b - M_u & p \\ -\Delta_1 & 0 & p & -\mu_d^b + M_d \end{pmatrix}$$

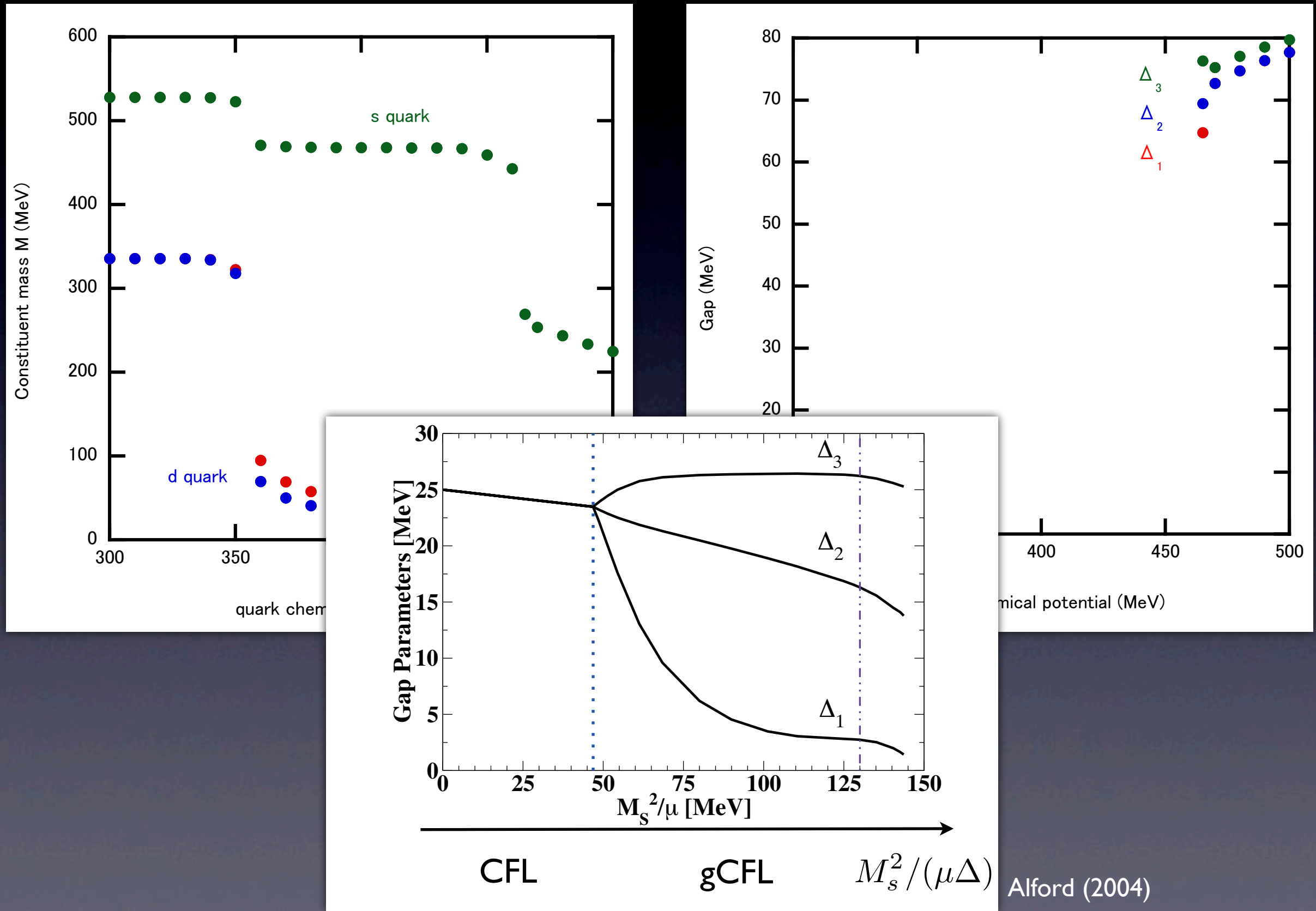
$$\begin{pmatrix} -\mu_u^r - M_u & p & 0 & 0 & 0 & 0 & -\Delta_3 & 0 & 0 & 0 & -\Delta_2 \\ p & -\mu_u^r + M_u & 0 & 0 & 0 & \Delta_3 & 0 & 0 & 0 & \Delta_2 & 0 \\ 0 & 0 & \mu_u^r - M_u & p & 0 & 0 & 0 & 0 & 0 & 0 & 0 \\ 0 & 0 & p & \mu_u^r + M_u & -\Delta_3 & 0 & 0 & 0 & -\Delta_2 & 0 & 0 \\ 0 & 0 & 0 & -\Delta_3 & -\mu_d^g - M_d & p & 0 & 0 & 0 & 0 & -\Delta_1 \\ 0 & 0 & \Delta_3 & 0 & p & -\mu_d^g + M_d & 0 & 0 & 0 & \Delta_1 & 0 \\ 0 & \Delta_3 & 0 & 0 & 0 & 0 & \mu_d^g - M_d & p & 0 & \Delta_1 & 0 \\ -\Delta_3 & 0 & 0 & 0 & 0 & 0 & p & \mu_d^g + M_d & -\Delta_1 & 0 & 0 \\ 0 & 0 & 0 & -\Delta_2 & 0 & 0 & 0 & -\Delta_1 & -\mu_s^b - M_s & 0 & 0 \\ 0 & 0 & \Delta_2 & 0 & 0 & 0 & \Delta_1 & 0 & p & -\mu_s^b + M_s & 0 \\ 0 & \Delta_2 & 0 & 0 & 0 & \Delta_1 & 0 & 0 & 0 & 0 & \mu_s^b - M_s \\ -\Delta_2 & 0 & 0 & 0 & -\Delta_1 & 0 & 0 & 0 & 0 & p & \mu_s^b + M_s \end{pmatrix}$$

Results (5): Case I

$$H = \frac{3}{4}G_s$$

12/16

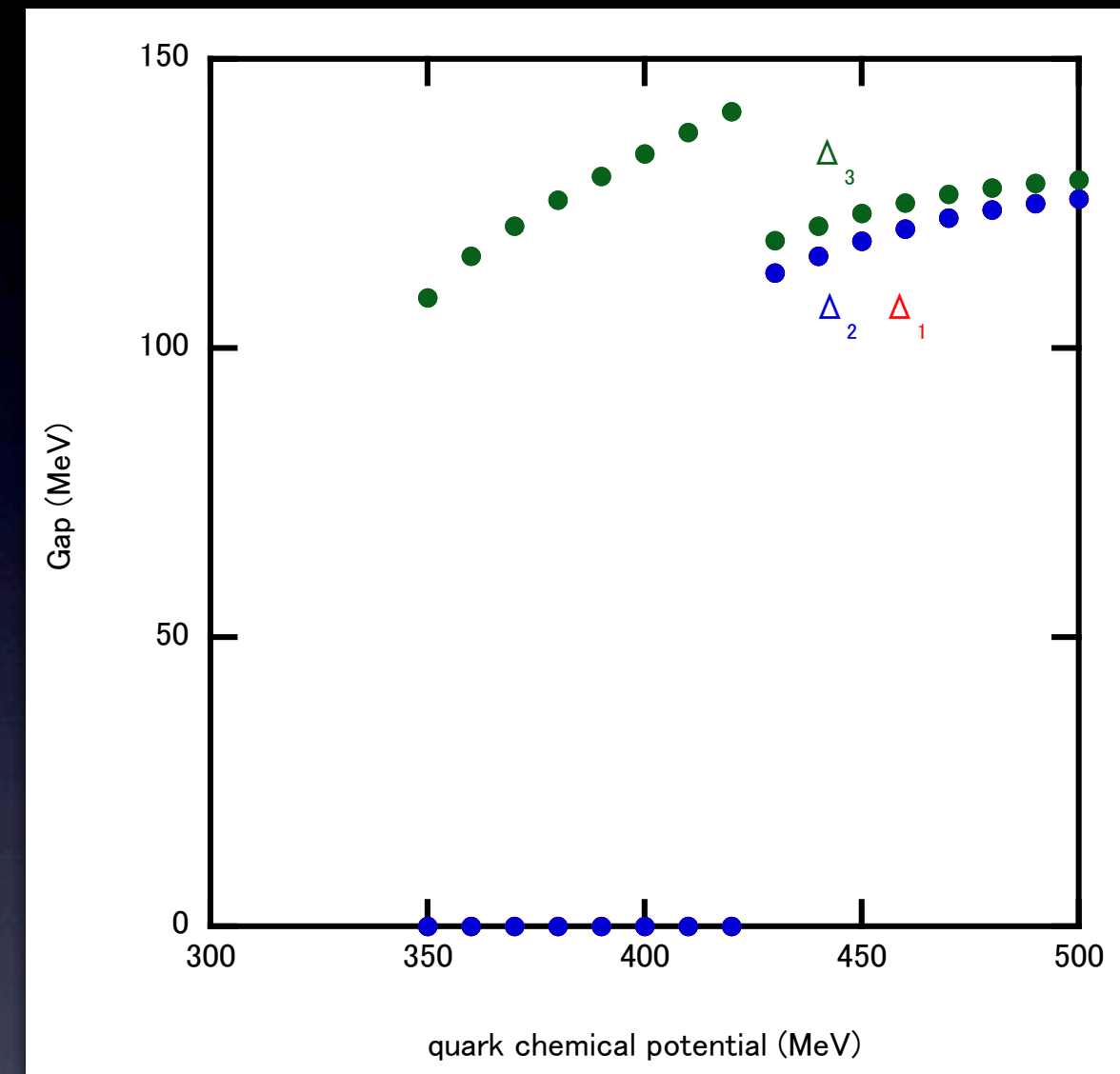
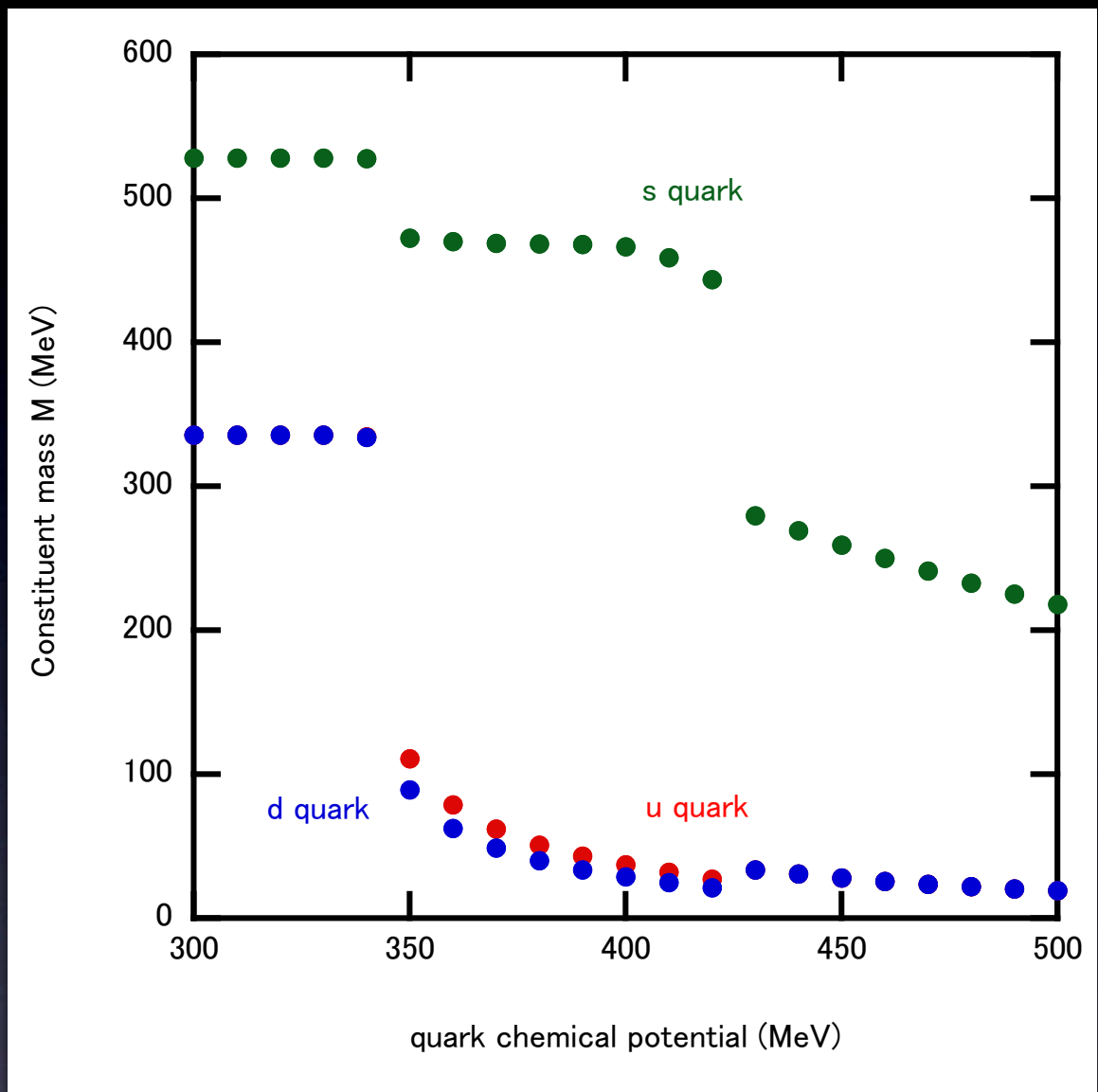
$g_v = 0$



Results (6): Case 2 $H = G_s$

13/16

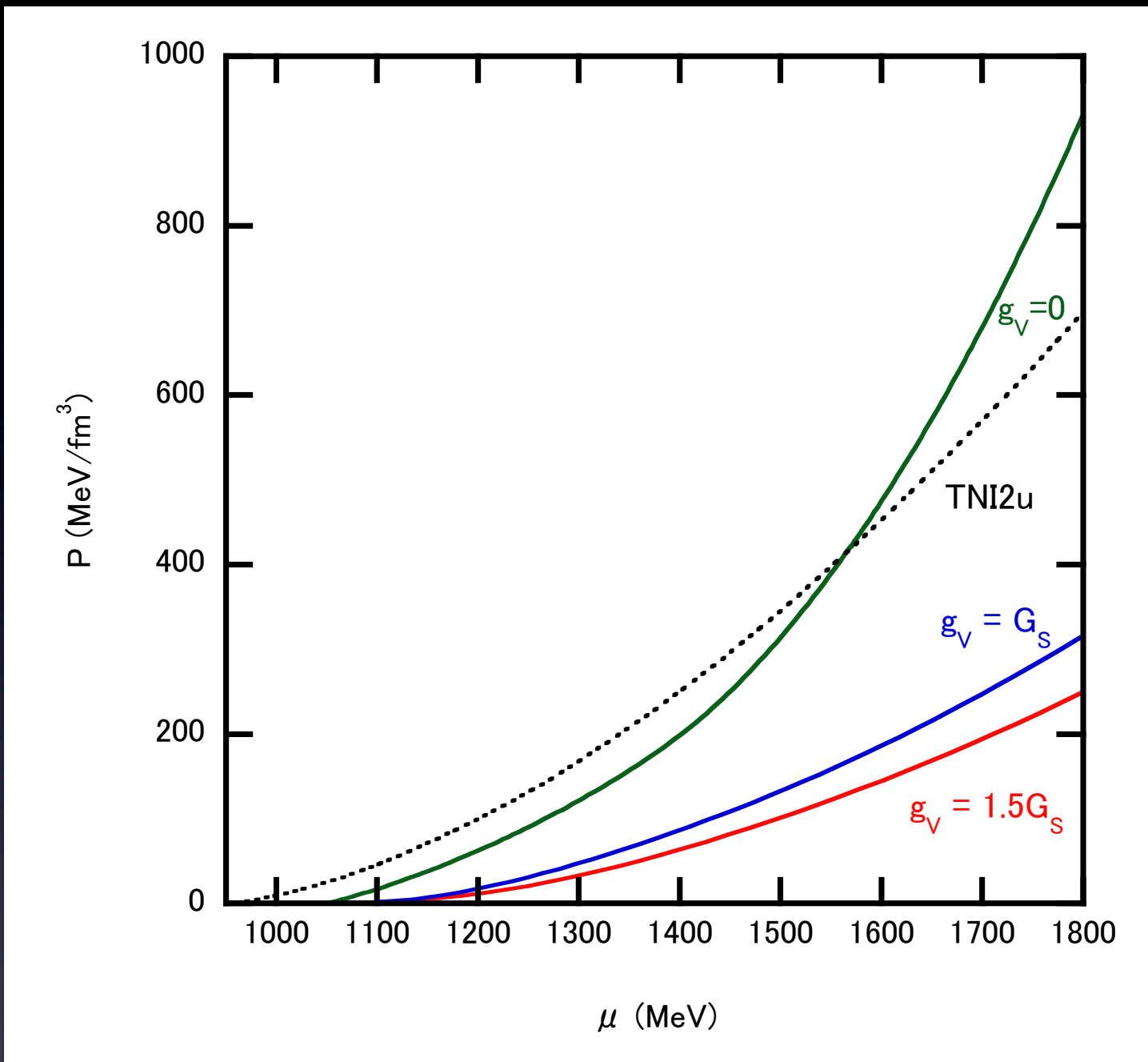
$g_v = 0$



2SC phase



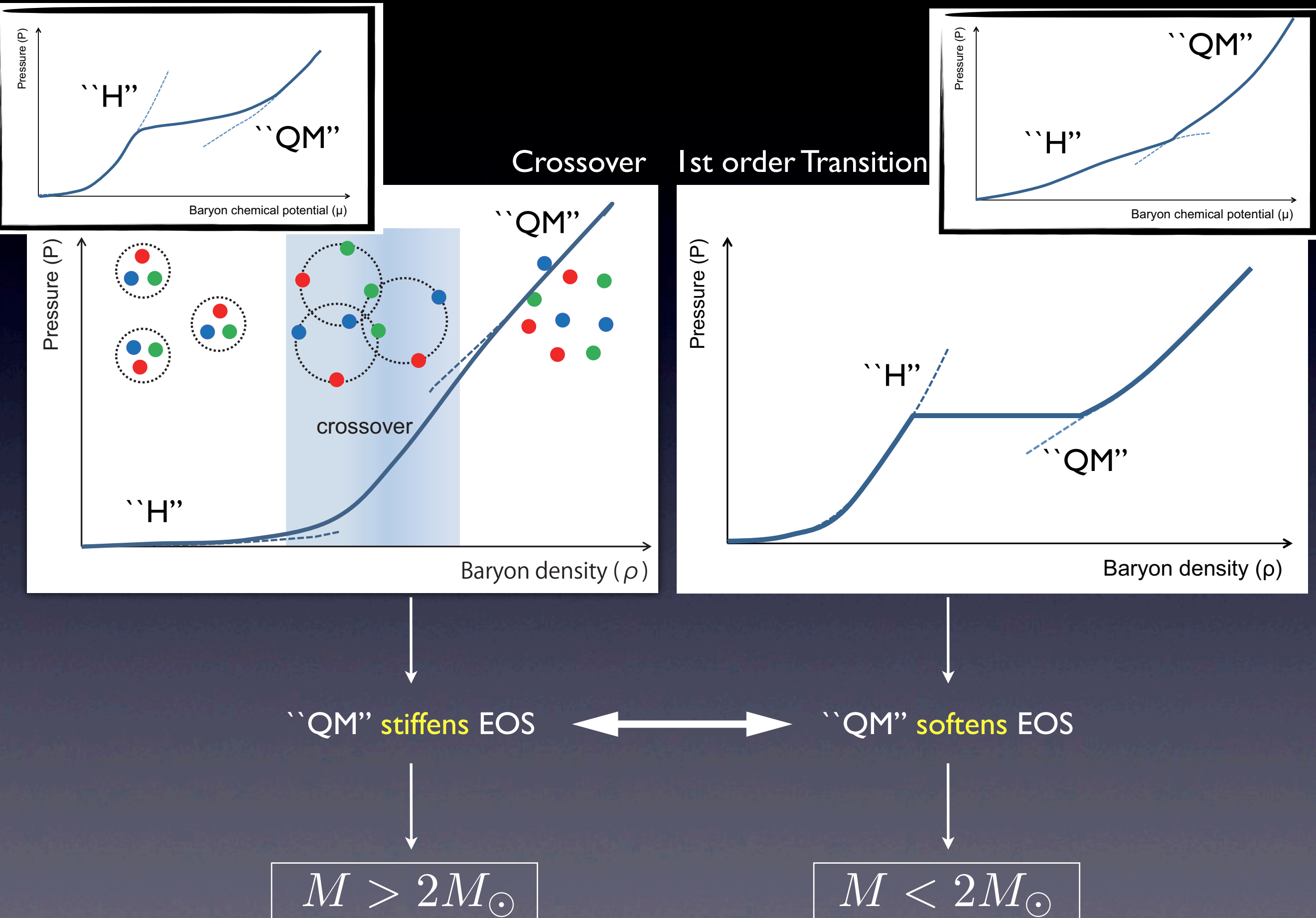
Crossover vs. 1st order Transition (Example)



In the case of $g_V = 1.0, 1.5G_S$, H-EOS and Q-EOS do not cross at all densities

Crossover vs. 1st order Transition

15/16



Neutron Star Observation

Observables:

binary period P_b

projection of the pulsar's semimajor axis on the line of sight $x \equiv a \sin i / c$ → mass function $f = \frac{(m_2 \sin i)^3}{M^2}$

eccentricity e

time of periastron T_0

longitude of periastron ω_0

+

General relativity effects:

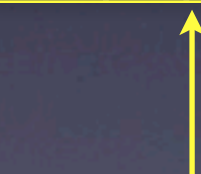
the advance of periastron of the orbit $\dot{\omega}$

Doppler + gravitational redshift γ

the orbital decay \dot{P}_b

range parameter r

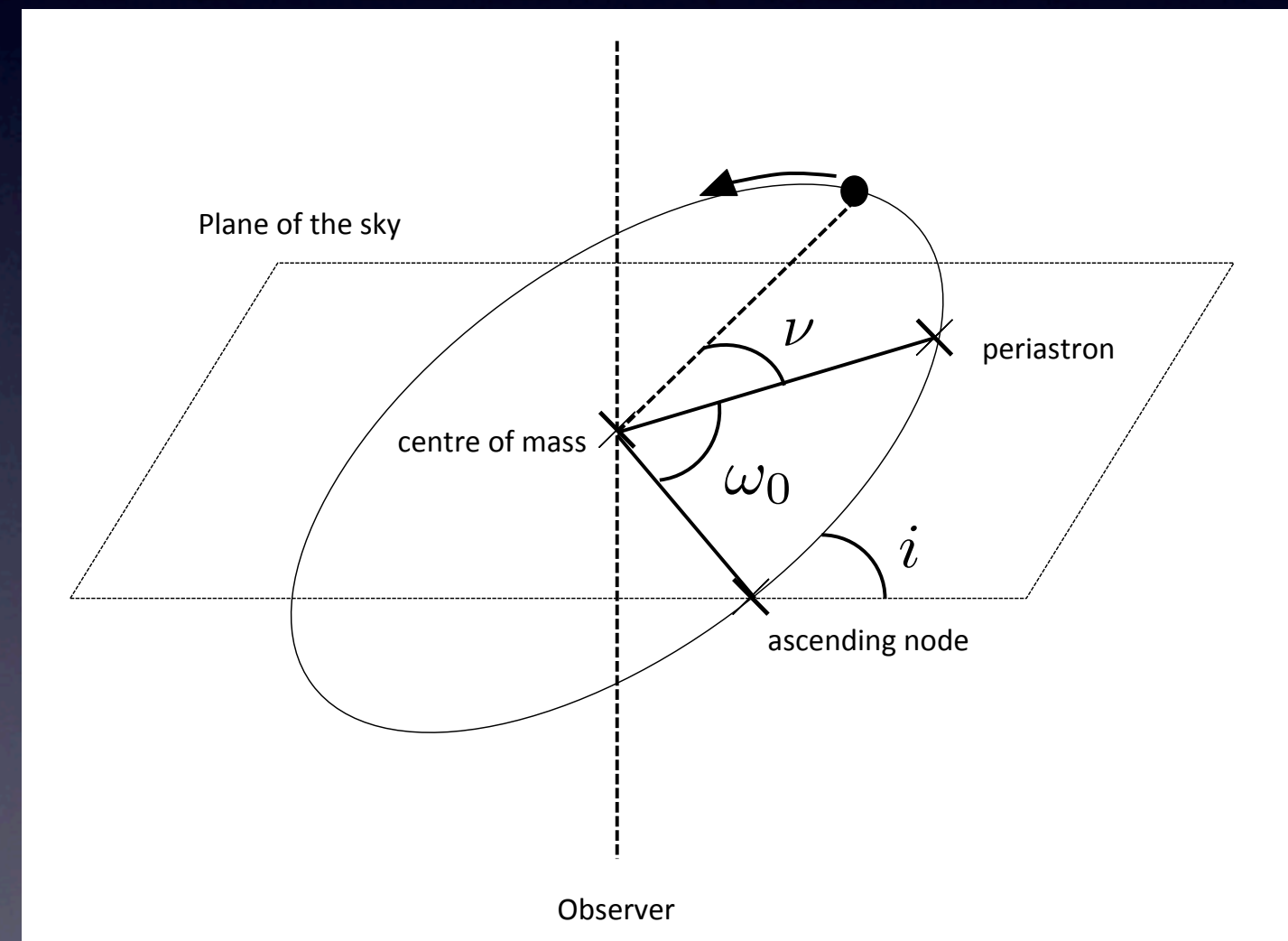
shape parameter s



$$\text{Shapiro delay: } \Delta = 2r \log \frac{1 + e \cos \nu}{1 - s \sin(\omega + \nu)}$$

Mass fraction $f + 2$ general relativity effects

→ Mass estimation



Universal 3-body force

TNI model

$$\begin{aligned}v_{TNI} &= v_{TNA} + v_{TNR} \\&= v_2 e^{-(r/\lambda_a)^2} \rho e^{-\eta_2 \rho} (\boldsymbol{\tau}_1 \cdot \boldsymbol{\tau}_2)^2 + v_1 e^{-(r/\lambda_r)^2} (1 - e^{-\eta_1 \rho})\end{aligned}$$

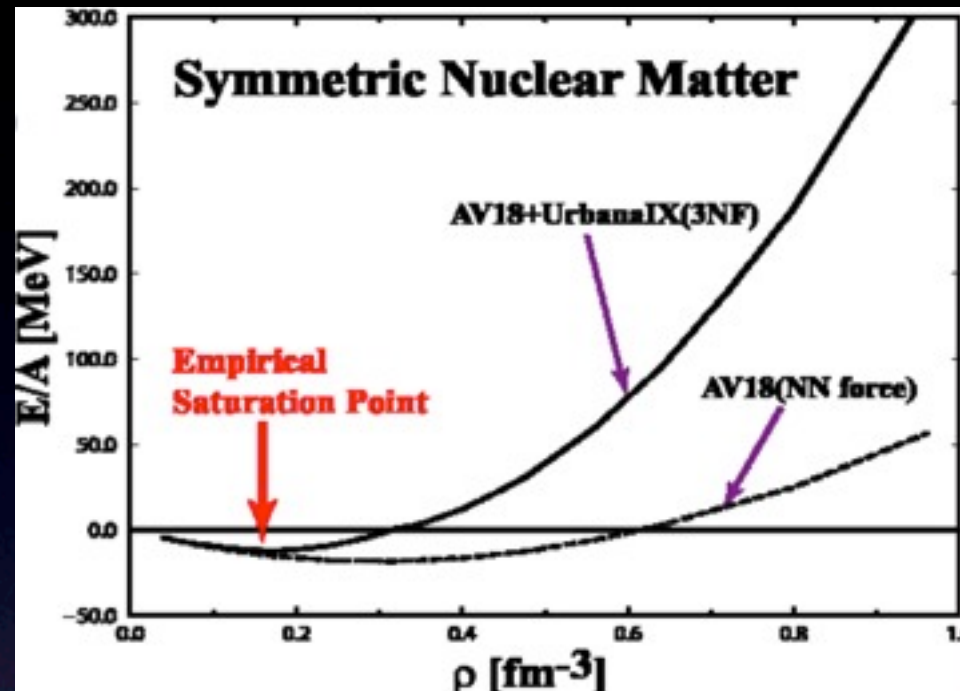
Urbana UIX model

$$\begin{aligned}v_{ijk} &= v_{ijk}^{2\pi} + v_{ijk}^R \\&= A \sum_{\text{cyc}} \left(\{X_{ij}, X_{jk}\} \{\boldsymbol{\tau}_i \cdot \boldsymbol{\tau}_j, \boldsymbol{\tau}_j \cdot \boldsymbol{\tau}_k\} + \frac{1}{4} [X_{ij}, X_{jk}] [\boldsymbol{\tau}_i \cdot \boldsymbol{\tau}_j, \boldsymbol{\tau}_j \cdot \boldsymbol{\tau}_k] \right) + U \sum_{\text{cyc}} T^2(r_{ij}) T^2(r_{jk})\end{aligned}$$

$$X_{ij} = Y(r_{ij}) \boldsymbol{\sigma}_i \cdot \boldsymbol{\sigma}_j + T(r_{ij}) S_{ij}$$

H-EOS: Universal 3-body force

3-body force is needed for saturation property



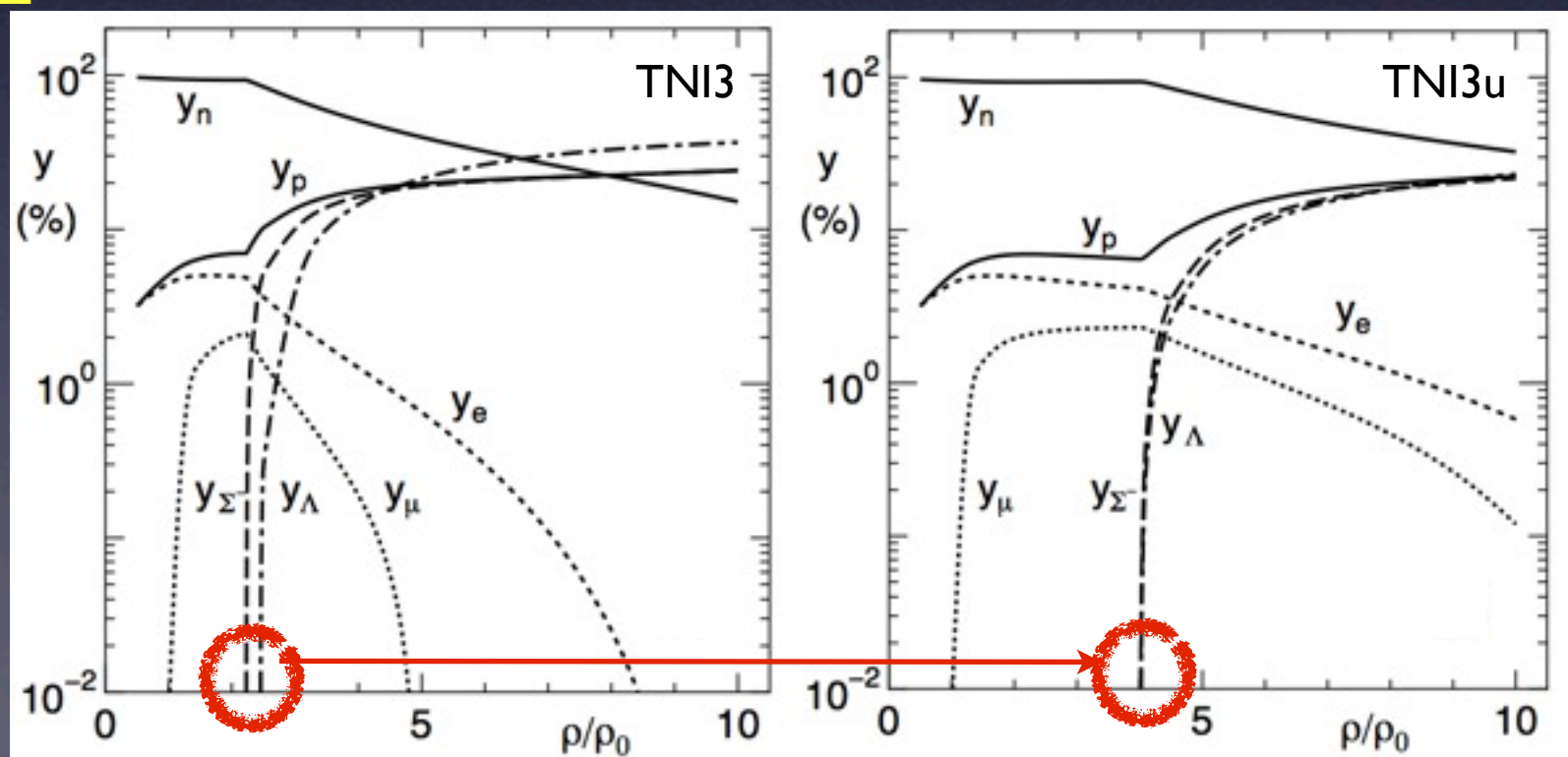
Akmal et al. (1998)

- From the point of view of NS observation, 3-body force is needed for the stiffness of EOS
- 3-body force between YN and YY can delay the appearance of the exotic components

Universal 3-body force

- TNI model:
G-matrix
NN : Reid soft-core potential
YN,YY: Nijmegen type-D hard-core potential

TNI2(3):
 $\kappa=250(300)\text{MeV}$



Nishizaki et al. (2002)

Cooling Problem

Rapid cooling is occurred by hyperons (Y-Durca)

$$\left\{ \begin{array}{l} \Lambda \rightarrow p + l + \bar{\nu}_l, \quad p + l \rightarrow \Lambda + \nu_l \\ \Sigma^- \rightarrow \Lambda + l + \bar{\nu}_l, \quad \Lambda + l \rightarrow \Sigma^- + \nu_l \end{array} \right.$$

